공학석사 학위논문

Study on the Current Density Distribution in Polymer Electrolyte Membrane Fuel Cell (PEMFC) System

고분자 전해질막 연료전지 내부

국소 전류 분포에 관한 연구

2020 년 8 월

서울대학교 대학원

기계공학부

이 영 호

Abstract

Study on the Current Density Distribution in Polymer Electrolyte Membrane Fuel Cell (PEMFC) System

Yeong Ho Lee

Mechanical Engineering

The Graduate School

Seoul National University

The fuel cell technology is in the spotlight as a next-generation energy source due to its relatively high energy conversion efficiency and storage capacity compared to other eco-friendly energy. In addition, numerous types of fuel cell is expected to be applied in various fields of industry, such as SOFCs for self-power generation, PEMFCs used for transportation due to its relatively low operating temperature. Not only

that, fuel cell technology is in the commercialization stage, the durability is considered as an important issue. Since, this study is studied about the local degradation and uniformity of current distribution to prevent degradation. The reffred local degradation can be occurred by temperature gradient which can be caused by different current density in the flow-field.

First, the experiment is conducted whilst adjusting the parameters when the fuel cell is under operation. As variables the operating temperature, humidity, and the flow rate of hydrogen and oxygen are changed. As an experimental method, the change in the current density distribution was examined by dividing the 25 cm^2 reaction area into 25 sections.

Second, a neural network is used to develop a model capable of predicting the 1) operating conditions of fuel cells from the current distribution and 2) the optimized operating condition from the current distribution data. To this end, various data pre-processing techniques specialized for the fuel cell have been applied and proposed. Also, a method for predicting operating conditions for controlling the current density distribution is newly introduced and verified.

Third of all, variation of current distribution when fuel cell is experienced degradation is also observed. To this end, an accelerated degradation techniques are introduced, and a phenomenon in which the degree of degradation is changed with humidity is observed. It is observed that the serious degradation is occurred near the outlet region by the level of humidity, and it is proved by several instruments such as EIS, SEM, and EDS. In addition, a new method is proposed to control the driving conditions through artificial neural networks to relieve the unbalanced current distribution. .

Table of Contents

List of Tables

List of Figures

Nomenclatures

c	specific heat (kJ/kg·K)
I	current (A)
V	Voltage
i	specific enthalpy (kJ/kg)
k	heat conductivity (W/mK)
P	pressure (kPa)
q	heat (W)
Q	flow rate (m^3/s)
T	temperature (K)
t	time(s)
u	velocity (m/s)
V	volume (m^3)
ρ	density (kg/m^3)

Subscript

amb	ambient
g	generation
MEA	membrane electrode assembly

Chapter 1. Introduction

1.1 Background of the study

As climate change is becoming a common global issue in the 21st century, the necessity of alternative energy sources is in the limelight. Not only that, but research about various substitution energy sources for fossil fuels are also ongoing in the fields of the energy industry for reducing the proportion of conventional energy source. Among them, the fuel cell technology emerges as the leader in the renewable and eco-friendly energy sector due to their unique characteristics and benefits. Fuel cells are believed to have been invented for the first time by Grove based on the electrolysis of water phenomenon in the 19th century. Since then, in addition to PEMFC using hydrogen and oxygen, other types of fuel cell such as SOFC and DMFC operating at different temperature ranges have been developed and used. These fuel cells are used in a variety of applications in different industries with their advantages.[1-3]

The applications and strengths of fuel cell technology to human society is significantly straightforward. First of all, it does not emit pollutants when it is under operation which can be related to any environmental issues. Second of all, the density of energy is relatively higher than other new types of eco-friendly energy sources such as solar power or wind power generation. Thus, it can supply the stronger power than other types of renewable energy.

Furthermore, it also can solve their chronic problems such as sustainability of solar panel in rainy days or reliability of power supply by a wind turbine in a mild climate region. For example, SOFC can be complemented domestic solar power system. The SOFC shows highest operation efficiency among the most type of fuel cells, but it operates normally in the vicinity of 600°C to 800°C in a relatively high-temperature range than other types of them. Therefore, PEMFC is using for the mobility industry, especially aimed to replace the internal combustion engine as a power source due to the low-temperature range for the operation. Aside from the public or private transport, it is using for military or entertainment purposes as well. For example, it is under development to replace an electric battery in the unmanned aerial vehicle (UAV) to extend the flyting time. Due to limitation of the capacity of the electrical battery and miniaturizing of it, PEMFC emerges as a replacement energy source for a longer flying time.

The components of a single fuel cell unit have consisted of five different parts; a pair of end and bipolar plates, gasket, gas diffusion layer (GDL) and membrane electrolyte assembly (MEA). Anodic and cathodic end plates are using for covering and containing the reaction parts of the fuel cell unit. Not only that, it generally carries a cooling or heating channel inside of them. Bipolar plates are designed to carry fuel and oxidant through the flow field in

Table 1. Hydrogen and fuel cell market overview (Ministry of Trade and Industry, 2019)

			2018	2022	2040
Hydrogen mobility	**FCEV**	**Cars**	1.8k	790k	5.9m
		Taxi	-		120k
		Bus	2	2k	60k
		Truck	-		120k
	Total		1.8k	81k	6.2m
	H_2 station		14	310	Above 1200
H_2 Energy	**Power Gen Fuel Cell**		307.6 MW	1.5 GW	Above 15 GW
	Household Fuel Cell		7 MW	50 MW	Above 2.1 GW
H_2 Productio	**Supply**		130k tons / yr	470k tons / yr	5.26m tons / yr
	Supply method		By-product H_2	+ Electrolysis	+ Import
	H_2 cost		-	6,000₩/kg	3,000₩/kg

them, so they can be regarded as a guided flow channel for the chemical reaction. Gaskets are placed between each component to prevent leakage of fuel and oxidant when they are under providing to fuel cell unit. In case of GDL, it supports that the fuel and oxidant to diffuse away as evenly distributed to the membrane. Lastly, the membrane has consisted of electrolyte and significantly tiny size platinum particles, catalysts, were applied on to the surface of it to promote the chemical reaction. Thereby, the electron moves along with the bypass current line what is connecting anode and cathode, and only H^2 ion can moves to cathodic plate through a membrane.[2]

Due to these reasons, PEMFC has several losses when it is under operation. Firstly, activation loss is one of a major loss for the activating the fuel cell reaction. For the chemical reaction, the specific energy is required which is bigger than the activation energy. Thus, the energy requirement for the stable reaction is an activation loss and the degree of the loss can be differed by states of membrane assembly (MEA) and operating parameters such as temperature, humidity and so forth. The second loss is an ohmic loss. It can be explained with a simple physical phenomenon as friction. When the subject moves much faster with the larger mass, the friction will be increased. In the same manner, an ohmic loss will be affected by the charge transfer and current flow. When the current flow is increased, normally the ohmic loss is also increased. The third major loss is concentration loss. It occurs from a lack of fuel or oxidant.

Table 2. Types of fuel cell (Fuel Cell Fundamentals, 3rd edition)

	AFC	MCFC	SOFC	PEMFC	PAFC
Operating Temperature (°C)	60 - 90	600 700	800 - 1000	25- 100	190 - 220
Generation Efficiency (%)	45 - 60	45 -60	50 -60	40 -60	40 - 50
Electolyte	Potassium hydroxide	Lithium	Yttria-Zirconia	Polymer membrane	Phosphoric acid
Catalyst	Platinum on carbon	Nickel	Zirconia cermet	Platinum on carbon	Platinum on PTFE

Increasing the current set variable requires the increment of fuel and oxidant to meet the minimum requirements for the high level of current. However, it is significantly difficult to maintain a steady and enough concentration of fuel in the outlet region. So, it is also should be handled for the better performance. Last but not least degradation factor is flooding. As a product of the electrochemical reaction, water will be created at the cathode side. This phenomenon could cause serious performance degradations, and also irreversible MEA degradation when it applied over-voltage unexpectedly.

Aside from the components of the fuel cell unit, several auxiliary systems are required to perform the fuel cell system. Firstly, fuel and air should be evenly supplied to the system for the stable operation condition. Second of all, each fuel and air should be humidified before the injection process to the fuel cell due to efficiency reason. Normally, fully humidified fuel and oxidant shows further improved performance than low humidity condition. Not only that, but precise measuring instruments are also required to monitor the temperature and pressure variation in the system. The reason for this is maintaining the constant temperature and pressure is an essential factor for stable operation.

For these reasons, PEMFC still has several limitations and challenges to be solved. Firstly, the total cost for the fuel cell system should be reduced. The cost of the membrane is still expensive due to the platinum catalysts on the surface. Besides, loads of auxiliary components are required to operate the

system, so it is not a positive case in terms of balances of plant (BOP) due to the volume of the whole system. Not only that, increasing the number of components and volume of the system, but it also leads to increasing the possibility of the fault of the system such as failure at gas providing system, humidifying system or temperature control system. Due to these failures, the performance of the fuel cell will be fluctuated, and the complexity of large BOP number will disturb the process of fault response. Not only that, but the membrane will also be degraded after long-time operation. Thus, this effect on the current distribution will also be identified.

For these reasons, the segmented fuel cell is used to figure out the performance variation due to fault or degradation. The segmented fuel cell can be observed current density distribution at the local points on the flow field. Therefore, it has used to determine the different unique characteristics depends on each auxiliary parts including degradation in the MEA. After experimenting, python based machine learning compiler is used for the experimental data processing to analyse the patterns of data variation.[3]

Finally, we identify the current distribution varies under the long term operation. Also, we examined the current distribution change along with MEA degradation as well.

1.2 Literature review

1.2.1 Current distribution in PEMFC

The amount of current drawing is not evenly distributed in all area on the MEA. It is changed and fluctuated by abovementioned factors; experimental conditions and xdFor these reasons, numerous researchers studied for solution plans and strategies for relieving these unbalance and degradation issues.[1-3]

Weng and Hsu [4] conducted a study on the local current density distribution with eight sections of segmented current measuring spots. In this study, various relative humidity conditions were tested to find out the tendancy of current distribution by operational parameters, and the performance of fuel cell near the outlet region shows higher performance than the inlet area due to sufficient amount of water as products of reaction and humidity conditions. Likewise, different humidity condition shows a different trend of current distribution.

Rajalakshmi and Raja [5] carried out the effect of humidification on the current distribution in the fuel cell. The research is about the evaluation of current distribution with a segmented fuel cell, and the used segmented fuel cell is separated into twelve sections. The current distribution with humidified reactants shows much even distribution than just ambient condition. Not only that, but the lower current condition also shows higher uniformity in current distribution than the high current condition.

Rui Lin and Jianxin [6] suggest the methods to improve the stability of a proton exchange membrane by optimization of relative humidity. The author states the stability of current distribution is significantly important due to it will induce the degradation of the cell. For this reason, several operating conditions are suggested to minimize the unbalanced current distribution in this paper. The essentially controlled factor is relative humidity and it is tested under 25% to 150% RH condition to the cathode side. According to this paper, the fuel cell has stabilized with optimizing the humidity of the anode and cathode, and also the oscillation of the current decreased by it.

1.2.2 Methodology for performance prediction with Neural Networks

A neural network is a network of neurons which are composed of artificial neurons. The connection between the nodes transmits the tensors to find an optimum solution or governing principle. In other words, these neural networks could be used for adaptive control, classification or prediction model for the dataset required industries. Due to analyzing the correlations between the datasets, it is possible to observe the trends which human cannot find. For these reasons, it is using for fuel cell technology as well, especially for prediction or adaptive control.

Belmokhtar and Agnoussou [7] used artificial neural networks for PEMFC modelling in their research. The method for predicting the PEMFC stack temperature under dynamic condition was suggested. This paper observed temperature variation under various driving conditions in between 27 to 45 V. Several driving conditions were simulated, and current and potential data used as a dataset. After several accuracy validations by choosing optimum hyperparameters, the tracking error for temperature prediction was reduced to less than 0.2%.

Chen and Laghrouche [8,9] also used an artificial neural network to predict the remaining useful life of PEMFC. The number used data type to build the neural network were five; stack current, stack temperature, air and hydrogen pressure, and air humidity. The dataset divided into two parts. The first part to train the neural network about the degradation of PEMFC and the rest of the data used to prediction and validation set. The mean relative error was less than 0.1 %, and neural networks provided highly accurate useful life prediction model. Not only that, but the degradation prediction is also improved as forecasting the degradation under the different operating condition with moving window method. The different moving window-sized led to different influence on the neural network performance, and each window size has compared to find the optimum prediction model.

Bicer and Dincer [10] used an artificial neural network to maximize the performance of the fuel cell. The research proposed a neural network model of 6 kW PEMFC, and the model was designed with experimental data to predict the appropriate outlet parameters. Furthermore, neural networks helped to predict and control the efficiency of fuel cell which is varying between the 20% to 60% of efficiency. According to the study, several essential hyper-parameters such as several hidden layers, training method and the number of samples were deliberately selected. After that, MATLAB model and neural network model have compared for the validation process. In the result, the author suggested the neural network as an alternative method to model a fuel cell particularly for the input and output combination case such as stack current, voltage or efficiency.

1.2.3 The variation of current distribution by MEA degradation

The PEMFC does not always perform in a steady-state condition. Due to the degradation of components, the performance of fuel cell reduces. Especially, the membrane contains carbon and platinum as a catalyst for the chemical reaction. Therefore, degradation in MEA is a significant problem for steady-state operation of the cell.

Eom and Cho [11] conducted an MEA degradation test with different materials of bipolar plates. For all materials, 1.4 V potential applied to the fuel cell under

open-circuit voltage condition as an accelerate stress test. In a result of the stress, the carbon in the membrane underwent corrosion and platinum catalyst agglomerated. For this reason, the performance of MEA reduced up to 30 % within the 20 stress cycle.

Shan and Lin [12] observed PEMFC performance degradation during dynamic driving cycle and overload condition. The variation of current distribution was shown in this paper, and the performance of it dramatically reduced after the 200^{th} driving cycle. In a result of this, the number of particles is reduced markedly in the inlet and outlet region compared to the middle region. However, some particles at the anode side did not change during the driving cycle due to it did not influence by flooding and chemical reaction. In the case of Pt particle size, aged MEA has a dash of bigger sized one, is a result of Pt agglomeration or migration. [13 – 16]

1.3 Objectives and scopes

Fuel cell research is now moving beyond the lab level to commercialization. Therefore, research on the durability and reliability of fuel cells will become gradually important. In the same manner, a fuel cell stack is a series of unit cells connected in series. Therefore, the fundamental research for improving the reliability is to predict the durability and degradation potential of the cell by observing the current density distribution in the unit cell.

In chapter 2, the unit cell experiment was conducted with various operating conditions. For measuring the local current densities, the segmented fuel cell was used, and the flow field type was a serpentine for both anode and cathode sides. The investigated operating conditions are the same as follow. Firstly, the operating temperature was controlled to understand the effects of temperature on the current distribution. Secondly, relative humidity (RH) condition was changed, and the stoichiometric ratio (SR) also tested to measure the variation of current distribution. These three factors are sensitively affected to the ohmic or concentration losses, and also different hydration or flooding condition led to totally different distributions [14 – 19].

In chapter 3, the neural network is applied to predict the current distribution of PEMFC. The research suggested a method to predict the high current and low current region under various operating conditions, and it expects to discover high local temperature area by drawing the amount of current density. Also, it can be used as an alternative of frequently using numerical modelling of unit PEMFC for the several benefits; identical accuracy, speed of calculation and flexibility. Along with the suggested neural network model, numerous other conditions which are not conducted in the experiment can be performed and simulated with a straightforward process. [20 – 24]

In chapter 4, acceleration stress test (AST) were conducted to investigate the variation of current distribution when it has degraded for several reasons;

ageing, reckless driving or overload condition. For fault mode simulation, one of well-known acceleration stress method, over-potential cycle, is applied. According to previous research, humidity condition or hydration is an essential factor to degrade the MEA in a fuel cell, so humidity condition and flooding effect are intensively focused as an experimental subject. Not only that, but the experimental process is also prolonged to validate the effects of water contents on the degradation with several experimental pieces of equipment such as HFR, SEM, EDS and TEM. Especially, inlet and outlet regions are compared for observing the different degree of degradation due to water contents by flooding effect. Not only that, different flow configurations, cross-flow and counter-flow, were tested to observe the influence of flow direction on the degradation. [25 – 29]

The purpose of this study is to clarify the correlation between current density distribution in a fuel cell according to operating conditions or degradation. Besides, a method of predicting and simulation using an artificial neural network is also presented to suggest a new type of fuel cell modelling. Overall, these concepts can lower the unbalancing of current and degradation issue to prolong the lifetime or reliability of PEMFC. [31 – 33]

Chapter 2. Characteristics of current density distribution under various conditions.

2.1 Introduction

As changing the operating condition of the fuel cell, current density distribution is varied. To achieve optimum or required fuel cell performance, the operation parameters can be controlled, such as increasing the pressure or temperature while reducing the humidity or air flowrates. This process can lead to changing in current density distribution, and it has several implications for the membrane or bipolar plates in the local degradation. In general, since the electrochemical reaction occurs more actively in the inlet region of the cell than in the outlet region, it is necessary to mitigate this unbalanced fuel cell performance in terms of the location of the chemical reaction.

To analyze this phenomenon, a segmented fuel cell was used for this study. The segmented fuel cell can measure the local current density along with the flow field in 25 spots, thereby measuring the change in the current density distribution according to the experimental condition. Therefore, the purpose of this study is to investigate the distributive of current density according to the operating condition and to propose a mechanism to prevent local degradation

to alleviate the phenomenon of rapid degradation in the high current density distribution region.

For comparing various operating condition, different air and fuel flow rates are tested while another factor is fixed. Furthermore, the effects of temperature and relative humidity of both sides are also observed. This chapter is divided into three parts; experimental setup, the process of experiment and results of each case.

In the experimental setup, the overall system configuration, the fundamental components of the fuel cell, and the components of the segmented fuel cell will be described in detail. In the experiment, process chapter will cover how the experiment was conducted in general and uncertainty analysis. In addition, the third conclusion will explain the current density distribution according to various fuel cell test conditions. As a result, a fuel cell operating method according to the purpose and optimal conditions will be presented.

2.2 Experimental setup

The experimental system consists of humidifiers, mass flow controllers (MFC) for each anode and cathode sides, unit fuel cell and heaters. The below figure 00 shows the schematic diagram of the used experimental system. As seen in the figure, the experimental system is designed with several auxiliary BOP systems for the operation. Firstly, the fuel providing system is placed on

the left side of the system. The hydrogen is provided from the hydrogen storage which is placed at the outside of the system. First, hydrogen and air are depressurized immediately before flowing into the system. Subsequently, the gas supplied at a set flow rate in the MFC is first humidified through a humidifier. After that, it is maintained at a predetermined temperature and then injected into the fuel cell.

2.2.1 Fuel cell components

Aside from the system, the unit fuel cell has several components such as end plates, bipolar plates, gaskets, GDL, and MEA. The below figures show the exploded view of the fuel cell unit. The used end and bipolar plates are made of carbon material, and the depth of flow-fields, anode and cathode, are different for the reason of reactivity of each gas. The depth of anode flow-field is 0.6 mm whilst 0.9 mm in the cathode. To seal, the gasket with a thickness of 290 ㎛ was used between each component; plates. In case of gas diffusion layer (GDL) is used to diffuse the fuel and air efficiently by deposited materials such as carbon and platinum, and it also helps to manage the water content ratio by different characteristics depends on the driving conditions. The used GDL model is 39BB made by CNL. Lastly, membrane electrolyte assembly (MEA) is a critical component for the exchange of proton between the anode and cathode. The role of the membrane is to allow only protons from the hydrogen

Figure 2.1. Experimental setup

Figure 2.2. Kikusui electronic load and MFC controller

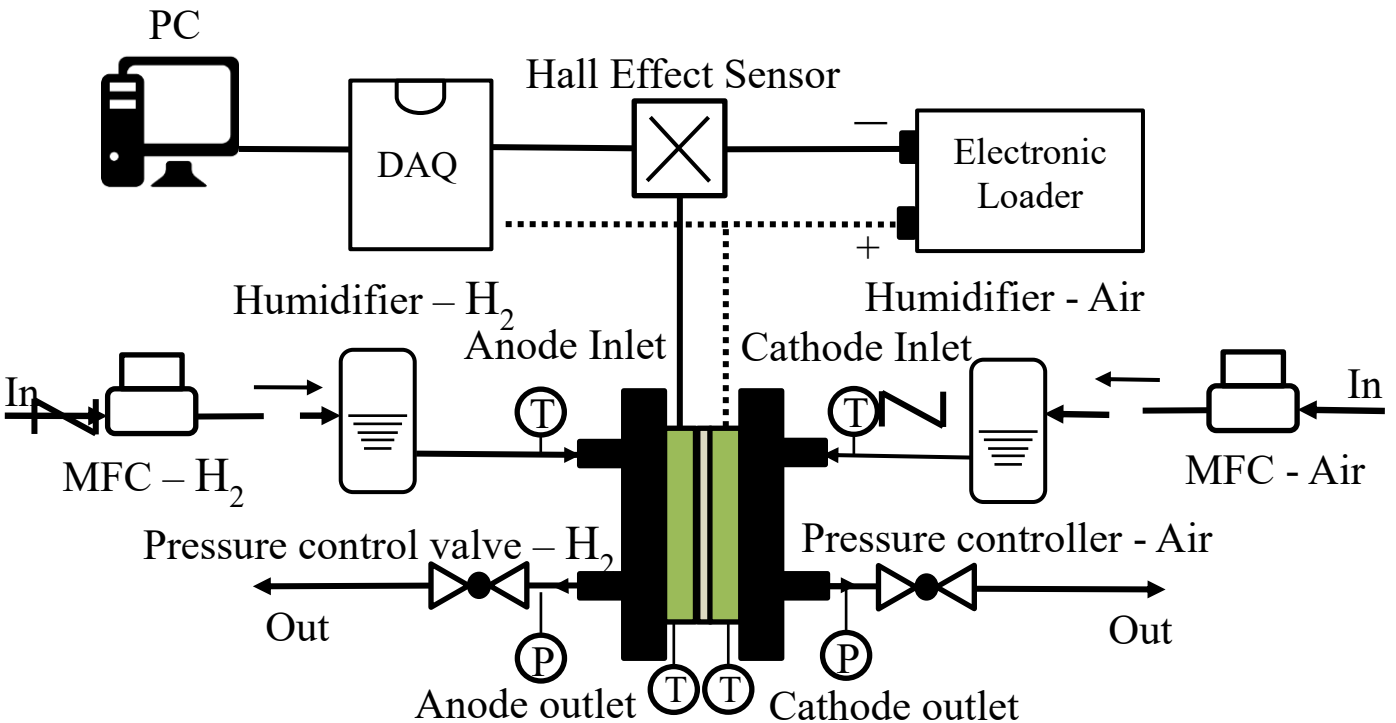

Figure 2.3. Schematic diagram of experimental setup

flowing at the anode to pass the membrane to produce electricity. Therefore, the membrane assembly has several layers which are catalyst layers at both anode and cathode sides and membrane itself. In addition, platinum and carbon-based catalysts are loaded on the surface to promote the chemical reaction and reduce the activation loss. The used MEA is designed and made by Vinatech, and it has a 25cm^2 active area, and 0.985 V at the open cathode voltage (OCV) condition.

2.2.2 Segmented fuel cell components

Several additional instruments and tools are required to measure the local current density distribution. Firstly, a hall effect sensor is a critical factor to experiment. The used hall effect sensors are clustered in 25 units which are able to convert the voltage signals into the specific ratio between 0 to 2 V. After then, it transmits the voltage data to the data acquisition (DAQ) in given converting ratio. The second component is a printed circuit board. The below Fig 2.5 shows the shape of the printed circuit board, and how it splits the flow-field into 25 local spaces. Hence, it can show the current density variations from the inlet to the outlet region when the operation condition changes or the MEA experiences the degradation. For the experiment, the multiple-layers printed circuit board is newly designed to minimize the difference of current losses, and it is stacked between the current collector and bipolar plate of the anode

Figure 2.4. A cluster of 25 hall effect sensors

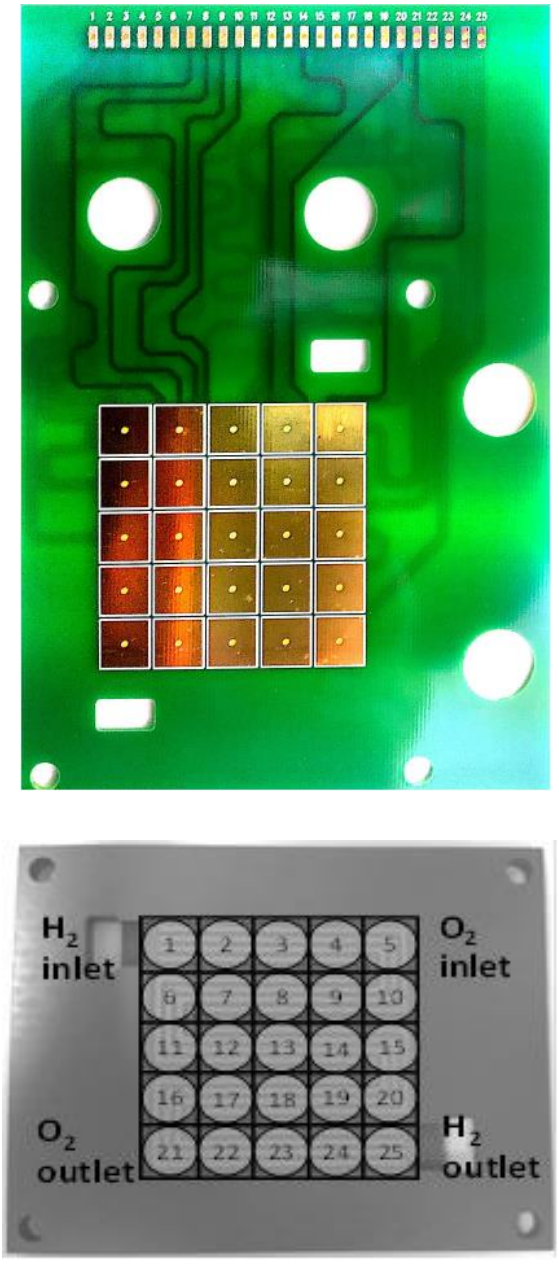

Figure 2.5. Printed Circuit Board (PCB) and segmented bipolar plate

side. The bipolar plate for the anode side is also newly designed. Due to all of 25 local spots are required to be electrically insulated, the serpentine flow-field is divided into 25 spots with electrical insulation. It then comes in contact with the printed circuit board and draws current into 25 current lines of equal length. Aside from current, it is essential to maintain the steady value of potential for all spots for the reason of sensing accuracy, voltage sensing lines are branched from the current line, and transmit to the data acquisition directly.

2.3 Process of experiment

2.3.1Experiment cases and conditions

Among various experiment cases, relative humidity (RH), flow rates (SR) and temperature are examined for the thesis. First of all, 20%, 40%, 60%, 80% and 100% for both anode and cathode side are tested. In the meantime, the temperature is fixed to 65°C, stoichiometry ratios are controlled 1.5 and 2.0 for anode and cathode sides respectively. For observing the effects of SR, anode SR are changed between 1.0 to 2.5 whilst cathode SR changed between 1.2 to 3.5. The other experiment condition is also fixed and the reference RH condition is maintained in 80% for both sides. Lastly, the temperature is also tested. The covered range is 50°C to 70°C for every 5°C. Same as previous cases, other conditions are fixed, and the only single parameter is controlled. The experimental cases are shown in below table 3.

Table 3 Specifications of experiment cases

Variable	Experimented parameters				
Temperature [°C]	50	55	60	65	70
SR_{AIR}	1.5		2.0		3.5
SR_{FUEL}	1.2		2.0		2.5
RH [%]	20	40	60	80	100

2.3.2 Experiment procedure

Before the set of every experiment, it is required to make the process for activating and conditioning the fuel cell to reach the standardized experimental conditions. Especially, the activation is processed under the fully humidified condition when the MEA is newly used for the whole new parameters. The reason for this is the water contents and hydration of the membrane are critical factors to decide the performance of the fuel cell. In case of electrical load cycle for the activation or conditioning, it consists of 2 minutes of OCV condition and 8 minutes of middle-range current and another 5 minutes for high range current. After the first cycle, the fuel cell is tested from the OCV condition to the maximum current density level in the cascade method. The determination of the completeness of activation is judged as the point at which the deviation is extremely reduced for each cycle. After it reaches a certain level, the experiment is conducted.

After the test preparation of the fuel cell is finished, the operating conditions are adjusted according to each experimental condition. In this chapter, the operating conditions are changed according to observe the characteristics of the current density distribution by temperature, flowrates, and humidity. Subsequently, changes in current and voltage are also observed from 0 A/cm^2 to $35A/cm^2$ under constant current conditions. Also, changes in current density distribution are observed through the segmented fuel cell.

2.4 Results and discussion

2.4.1 Relative humidity

Among various parameters, humidity condition is tested as a first condition. The tested RH conditions are 20%, 40%, 60% 80% and 100% for both anode and cathode sides as shown in the previous table 3. The below figure 6 shows the voltage and the maximum power density variation along with the current changes. Current density is controlled from OCV condition to 1.5 A/cm2 at every 0.1A/cm2. As shown in the graph, the maximum power density is shown in the vicinity of 1.2 A/cm2 and it decreased due to mass transport loss. It results from the reduce in reactant concentration at the surface of the electrode.

In terms of fuel and air concentration, fuel and air shortage at the high current region is a primary reason that causes the transport loss. In the case of the second reason, water is a product of the operation of the fuel cell, and it is retained in the outlet region as a disturbance of reaction. Therefore, we can observe the concentration loss remarkably at the high current region as seen in the below Fig 2.6.

If we take a closer observation at the effect on humidity, it shows a huge difference between the conditions as shown in Fig 2.7. In low humidity condition, the reaction rate at the inlet area is not sufficient due to lack of hydration and humidity at both sides. However, flowing with the flow-channel

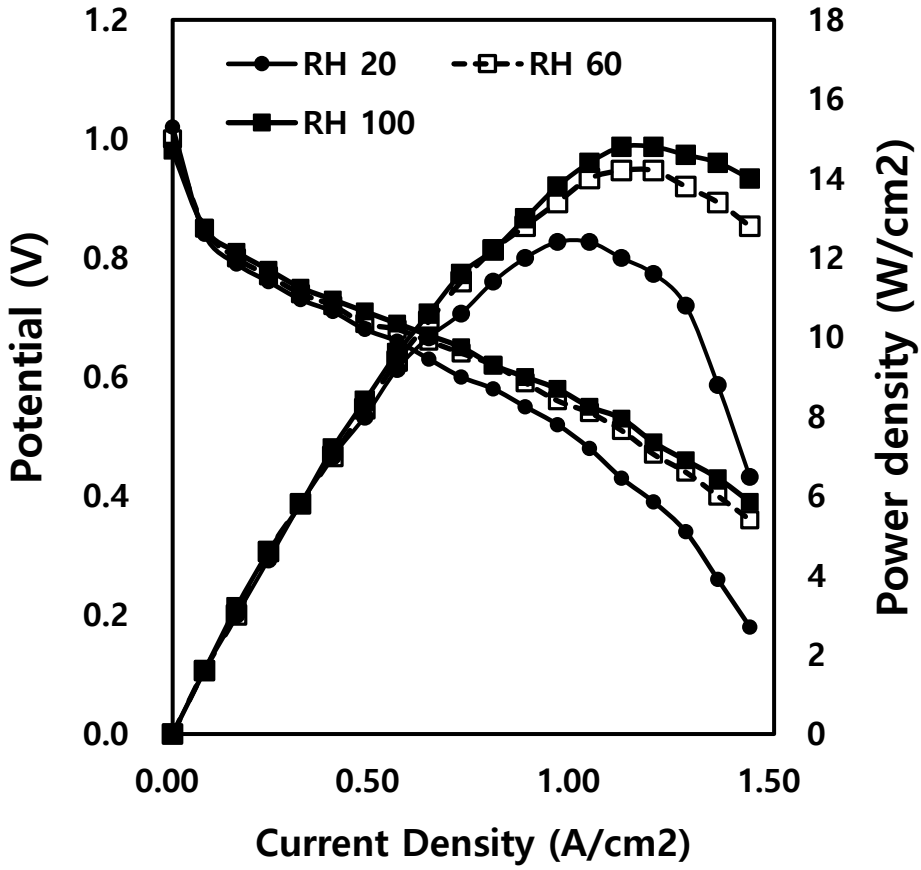

Figure 2.6. IV and IP curves at different humidity condition

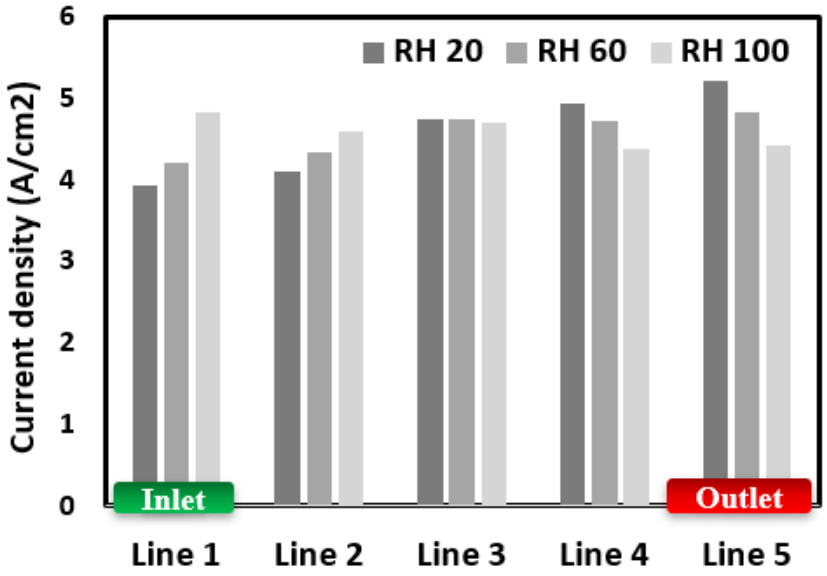

Figure 2.7. Variations of current density distribution when humidity condition changes

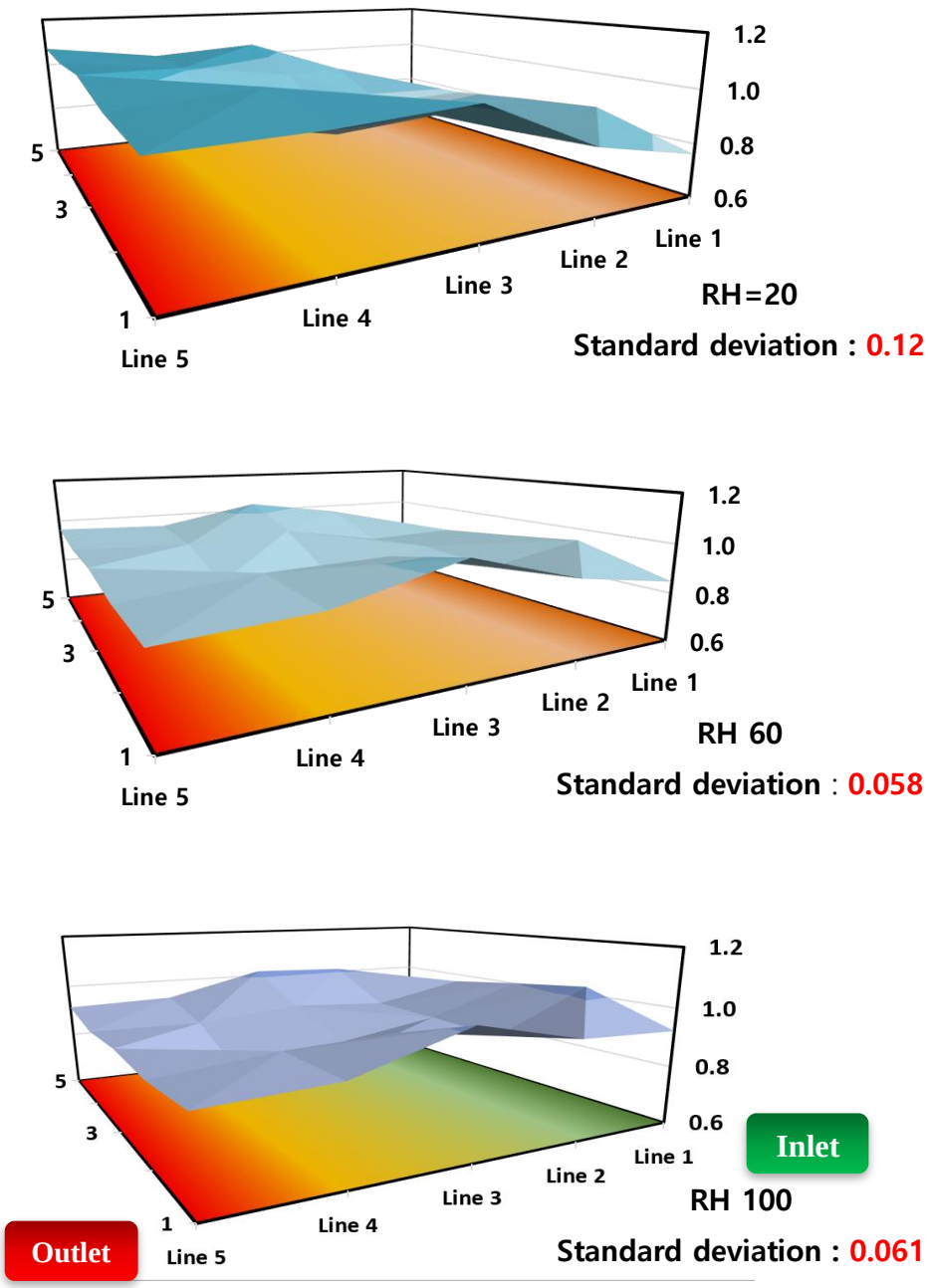

Figure 2.8. Variations of current density distribution and standard deviation in 3D projection

provides water as a product. Hence, it reaches the level of the current condition in terms of total power output. The reason for this is that the inlet region is not operated appropriately due to low humidity condition. Not only that, if the flooding occurs at outlet region in low humidity condition, but inlet and outlet both regions also do not operate in stable condition, so it shows the lowest power density. In the case of high humidity condition, the air and fuel are provided immediately from the inlet region, so it shows higher power density than the low humidity condition. This is because high humidity conditions allow drawing the current from the inlet region immediately, so mass transport loss is decreased as shown in Fig 2.6**.**

Aside from the unit cell, Fig 2.7 shows local current density distribution when humidity condition changes. As mentioned above, under insufficient humidification, the current density at the inlet area is about 30% smaller than the outlet region. As the level of humidification increases, the current density distribution is gradually became uniform, and when it reached about 80%, it shows an almost similar tendancy with the 100% humidification. Therefore, for the efficient operation of the fuel cell, it is not necessary to operate under the humidity condition of RH 80% or higher, in terms of maximum performance or current density distribution.

In case of standard deviation, Fig 2.8 shows how the uniformity has changed along with the RH condition. Due to unbalanced current distribution yields

local degradation by unbalanced heat generation, it is necessary to prevent the degradation by operation conditions. As shown in Fig 2.7, uniformity of current distribution reaches the lowest point between the RH 60% and 80% condition, and increased again in fully humidified condition. The reason for this is low RH condition is not sufficient to accelerate the reaction in the inlet region, so it has the highest standard deviation. In case of fully humidified condition, it shows the most serious flooding effect at the outlet region. Hence, the reaction at near outlet shows relatively low current distribution than the inlet region. Therefore, if the fuel cell requires to operate under uniform current distribution, RH 60% and 80% are recommendable. However, if it is necessary to perform with maximum output, RH 80% would be the optimum condition for driving.

2.4.2 Stoichiometric ratio

The stoichiometric ratio defines the exact ratio between the air and reactant gas for the sufficient amount of power generation such as relations between the actual consuming amount and required amount. For an investigation of effects on SR to the performance and current distribution, air and fuel flow rates are adjusted separately. The minimum threshold flowrates for the anode side is 1, so 1, 1.5 and 2.0 in SR for the anode side is tested.

Firstly, fuel providing rates are controlled to observe the effect on the performance of anode SR. Due to minimum requirements to perform, SR of the fuel side is tested from 1.2. As shown in Fig. 2.9, increasing SR in the anode side leads to influence to the mass transfer loss, but it did not elevate the maximum performance remarkably. The reason for this is the reactant rates of hydrogen is extremely faster than the cathode side, and the air flowrate is a dominant factor to control the maximum performance than the anode side. As seen in Fig 2.10 the maximum power output is increased by about 70% from the lowest air SR, 1.2, to the air SR in 3.5. From the calculation, it is required to provide fuel and air at least 1.0 and 2.0 to draw current in 1.0 A/cm^2 in the stable. Therefore, Cathode SR in 1.2 shows the largest mass transfer loss. In the case of air supply in larger SR, it reduces the mass transfer loss remarkably due to the sufficient amount of air concentration · parts in the flow field.

Aside from the entire unit cell, Fig 2.11 shows local current density distribution when fuel providing changes. As mentioned before, the hydrogen reaction rate is extremely fast, and it is not a critical factor to change the performance and distribution unless it is larger than the minimum requirements. Therefore, the current distribution does not change remarkably. In the case of air provides, it shows larger changes than the anode side. Fig 2.12 shows the variation of current distribution when the SR of air increases. In low air SR condition, most of the reaction is occurred in the vicinity of the inlet region due to the shortage of fuel at the outlet region. Hence, the uniformity of the current is extremely low than in the other two cases. As following cases, air SR in 2.0 and 3,5 shows the further uniformed current distribution by relieving the mass transfer loss issue. However, the uniformity of SR2.0 and 3.5 shows an almost identical trend, so it can result in the air providing in SR 2.0 is sufficient to perform 5 by 5 size fuel cell.

To observe the uniformity further in detail, Fig. 2.13 shows the variation of a standard deviation when SR changes for both sides. Firstly, the standard deviation in the anode side does not change significantly as mentioned before. However, airflow rates derived huge different in standard deviation as the level of cathode SR changes. Increasing in cathode SR reduces the standard deviation, but the maximum uniformity is shown in the vicinity of 2.0

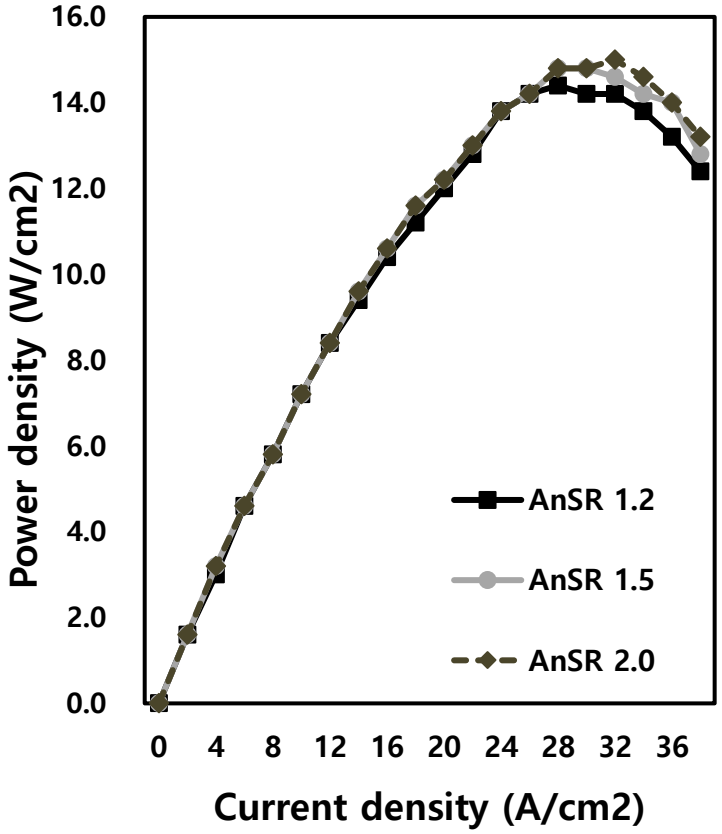

Figure 2.9. IV and IP curves with changing fuel providing

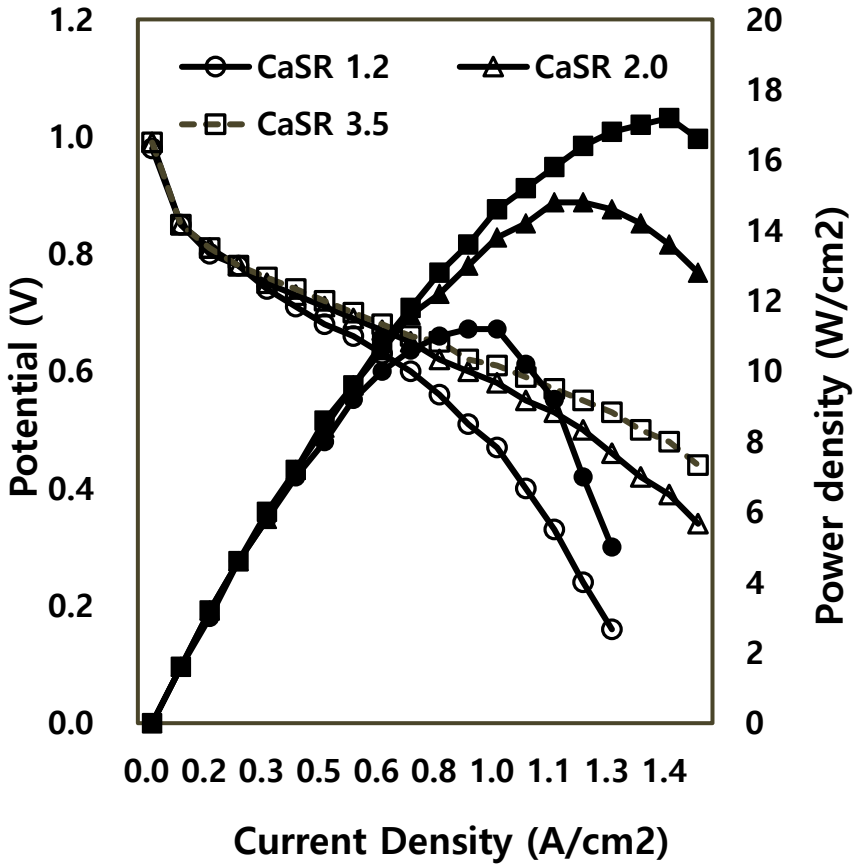

Figure 2.10. IV and IP curves with changing air providing

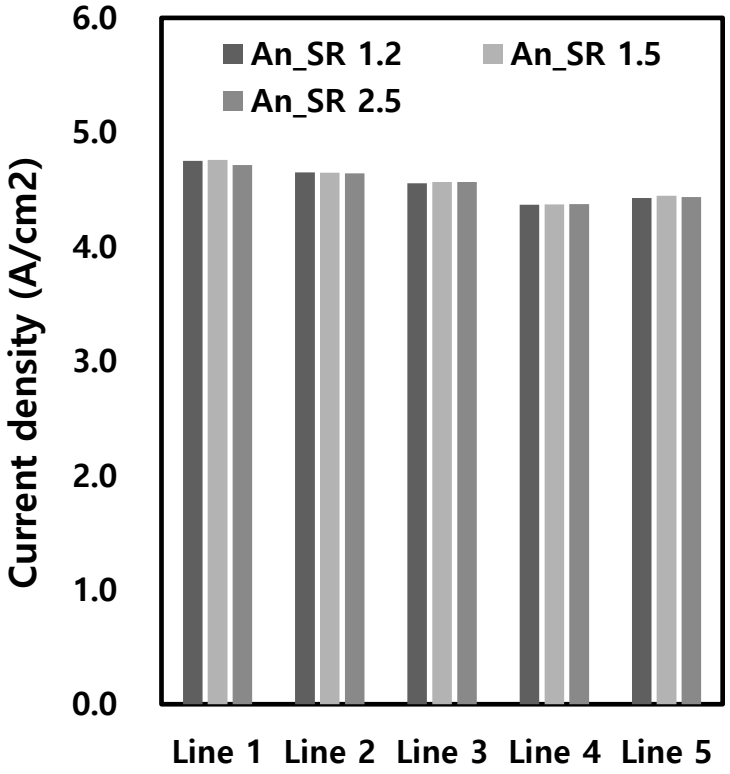

Figure 2.11. Variations of current density distribution when fuel providing changes

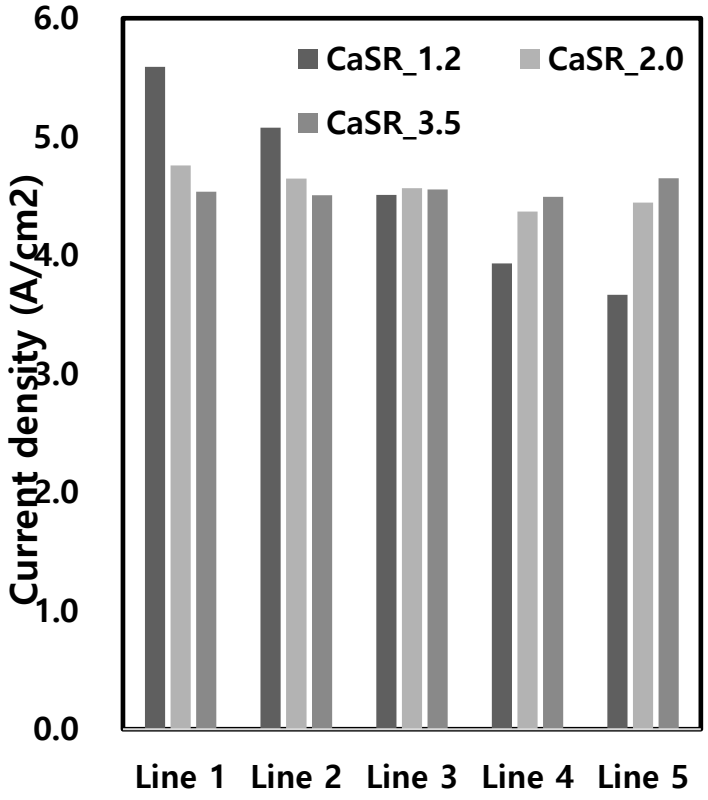

Figure 2.12. Variations of current density distribution when air providing changes

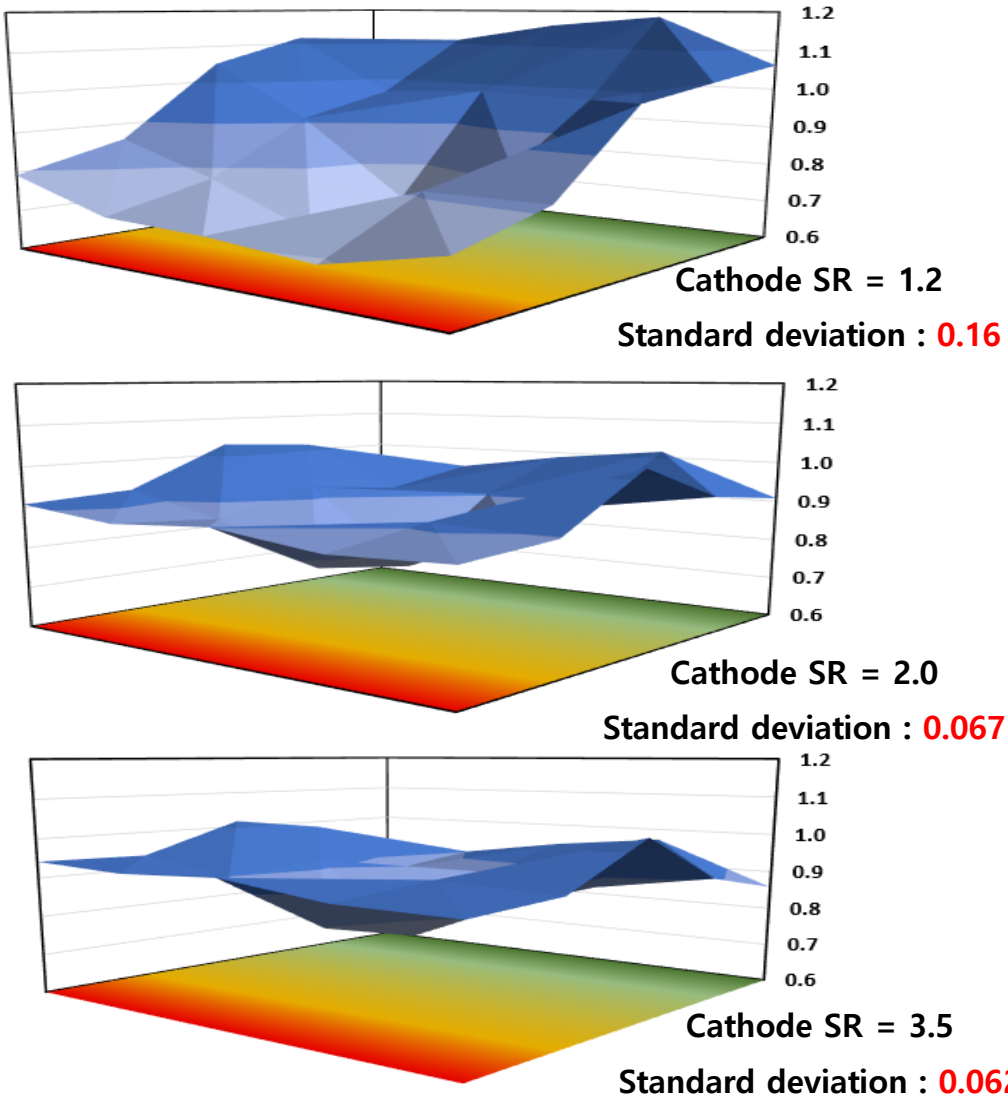

Figure 2.13. Variations of current density distribution and standard deviation in 3D projection when air providing changes

2.4.3 Temperature

As abovementioned, polymer electrolyte membrane fuel cell (PEMFC) performs in a relatively low-temperature range such as 60°C to 100°C. For this reason, it is critical to find the optimum operating temperature to cut off the thermal energy loss and extend the lifespan of the membrane. The tested temperature range is between 50°C to 70°C in every 5°C. Generally, PEMFC is operating at 60°C to 70°C except for the high-temperature PEMFC for the reason for optimization. Therefore, in that temperature range is observed in detail.

Fig 2.14 shows the overall performance of fuel cell by temperature increasing. Due to the low-temperature range, 50°C shows the lowest power output among all conditions. After 60°C**,** maximum power output is reached to similar power output with other higher temperatures, but it is still plotted at the slightly lower point. At 65°C and 70°C show the almost identical power output, so it can be regarded as it is not necessary to heat the fuel cell above than 65°C unless the fuel cell is required to perform as a high-temperature PEMFC.

In the case of local current distribution, Fig 2.15 shows the variation of it by changing the temperature. Due to the other experiment condition is fixed to reference condition, relative humidity is set to 80% which is relatively high

humidity condition. Hence, the current density at the inlet region is higher than the outlet region as explained before. Not only that, but the temperature also does not affect on the current distribution seriously than other conditions. It has changed slightly, but it does not show dramatical tendancy changes such as humidity or SR conditions.

However, if we focus on the standard deviation, it is possible to find the difference. Fig 2.16 shows the variation of standard deviation along with increasing temperature in the tested current range. As shown in the figure, in the vicinity of 60°C denotes lowest standard deviation which is only about 70% of the biggest deviation in 70°C. In addition, the results did not appear linearly, but even at around 50°C, the uniformity is shown as extremely low due to insufficient reactivity. This shoed similar results to the lowest uniformity case which is 70°C. Therefore, if we consider the efficiency when operating a fuel cell, it can be determined that it is most suitable to operate at 65°C, but if we need to operate with a uniform current distribution, 60°C would be a better condition.

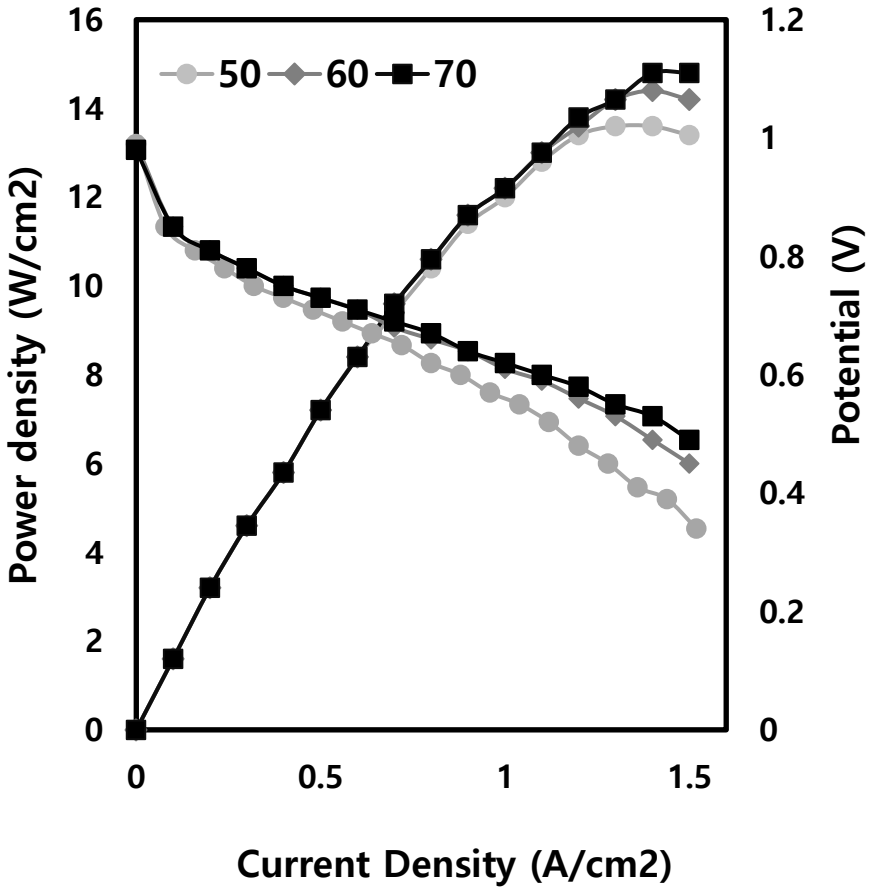

Figure 2.14. IV and IP curves with changing temperature

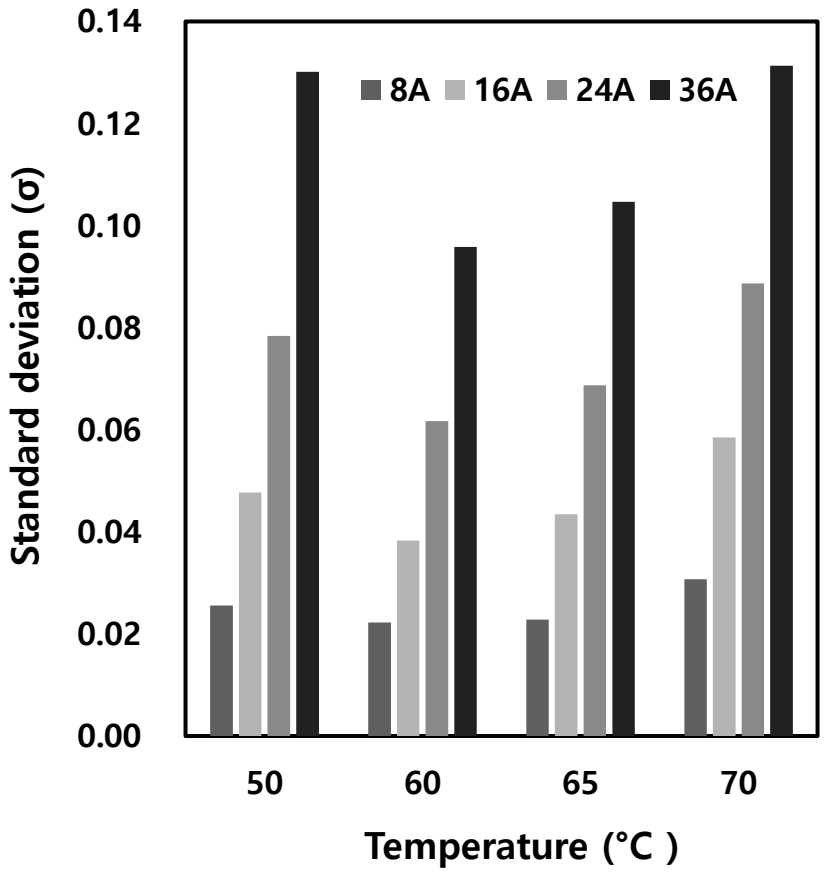

Figure 2.16. Variations of standard deviation with changing temperature and current density

Summary

In summary, the fundamental factor to change the performance and current distribution of PEMFC is operating parameters. In addition, the current distribution is a promising issue for the reason of the reliability of fuel cell. According to previous research, unbalanced current distribution leads to local degradation by unbalanced thermal shocks. Therefore, it is required to observe the variation of current distribution under various operating conditions. Firstly, the humidity condition is tested. The results show the highest current region can be shifted by changing the humidity condition from the outlet region to the inlet region due to the reactivity and flooding effect. Along with maximum power output, 80% RH condition for both sides can perform as fully humidified condition, and the vicinity of 60% shows the most uniform current distribution. In the case of stoichiometric ratio (SR), over-providing of fuel does not influence the distribution unless it reaches minimum threshold flowrates. However, air flowrates are effected on the uniformity instantly due to its reaction rate. Lastly, the temperature is tested between 50°C to 70°C, and maximum power output is performed in 65 to 70°C whilst optimum uniformity is found at 60°C.

Chapter 3. Neural network-based prediction model for current density distribution in PEMFC

3.1 Introduction

Machine learning and deep learning technologies have attracted attention as a promising technology since the 2010s. Accordingly, this technology is breaking down the technological boundaries between its own disciplines, and further introducing them for the development of different fields. In this regard, fuel cell industries also attempted to apply it to the fuel cell system, especially for the fault diagnosis purpose. Aside from the reliability engineering, this study is started from the consideration of the technological convergence between the neural network and fuel cell unit. As fuel cell technology is in the commercialization stage, it is a critical factor to observe the current density distribution due to unbalanced current density distribution.

The purposes of using the neural network are divided into two main categories. The first purpose is building the neural network which is possible to predict the current density distribution under various conditions. The existing method to predict the current distribution is numerical modelling. However, the previous designed numerical modelling shows relatively low accuracy to simulate the current density distribution. The reason for this is the calculation

for the local water contents of Nafion, heat flux, and concentration of gases are extremely difficult to compute with high accuracy. Even if it succeeds, the computation time will take about a few hours to days to calculate for just a single case of distribution. In this regards, the neural network is suggested to complement this issue. About 60 datasets are obtained by experiment with changing the parameters. After then, the neural network is designed with several data pre-processing steps.

The second purpose of using neural network is finding the optimum driving condition to make the current distribution uniformly. To achieve this, the previous neural network is re-designed by several techniques, and the suggested conditions are validated by a previously designed neural network.

3.2 Process of modelling

3.2.1 Data preprocessing techniques

There are several requirements for a neural network to perform with high accuracy. The first condition is that the data being trained or tested must be within a certain range. Therefore, the first pre-processing technique is using a tool to scale down the local current into -0.5 to 0.5 range. The second technique is to set the experimental values with slight fluctuating to a steady value by considering the ratio. To achieve this, all the set variables are converted into 25A. The third technique is the consideration of other operating parameters

such as temperature, pressure, flowrates and relative humidity. All of the parameters are on a different scale, it is necessary to scale down or up the parameters into a certain region. Therefore, scalers designed in different methods were used to collect the scattered data within a certain range. Not only that, several techniques are also suggested to the fuel cell system such as filtering the key factors to build the neural network and so forth.

3.2.2 Selection of hyperparameters

When building the neural network, it is an essential process to select proper hyper-parameters. There are several main parameters that the factors are required to adjust in detail.

The first hyper-parameter is the size of the hidden layer. The hidden layer is a series of nodes, combined with nodes that look like neurons in the human brain. The shape of the neural network is shown in Fig 3.1. According to previous studies, it is effective to set the number of nodes in the first layer of the neural network to a number similar to the number of input data. Thereafter, the number of layers of the second and subsequent layers should be sequentially reduced according to the number of the desired number of outputs. In the case of the number of output is more than the number of input, unlike the previous example, the size of the hidden layer must be increased sequentially. For example, in the case of the first neural network to predict the current density

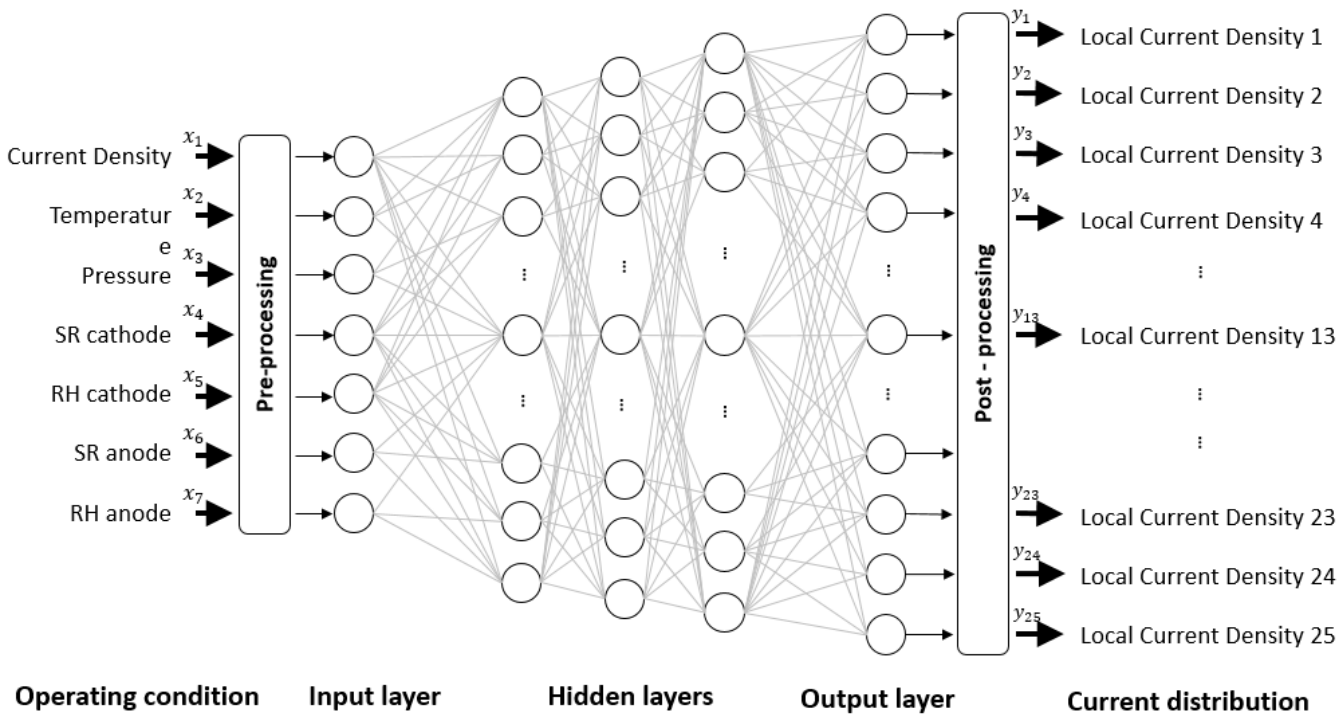

Figure 3.1 Shape of current prediction model based on neural network

distribution from the operation conditions, the size of hidden layers is 10, 15 and 20 as increment direction. However, the secondly suggested neural network which is built for suggesting the optimum operation parameter, the hidden layer size is 20, 15 and 10 as a counter-direction of the previous one.

Second hyper-parameter is learning rates. The optimization of learning rates can find the solution of the structure of data in terms of the gradient descent method. For example, the gradient descent method is similar to the lost in the mountain valley. When a hiker lost their way near the peak of the mountain, the primary step should be taken is walking down to the downhill. However, it is difficult to find the way to lowest spot without a compass. Not only that, but we also do not know the arrived place after few hours of walking down is the lowest point. Likewise, finding the optimum learning rates is similar to giving the compass and coordinate of the lowest point to the neural network. The below equation shows how the algorithm find the solution.

$$\theta j = \theta j - \alpha \frac{1}{m} \sum_{i=1}^{m} \left(h\left(x^i\right) - y^i \right) x^i$$

The above equation leads to find the direction of the search of the lowest point. It updates the theta value continuously by iteration until finding the lowest convergence point. Therefore, about ten learning rates were tested to find the optimum convergence value.

There are a few more hyper-parameters, but the last main hyper-parameter is batch size. Due to massive data size, it is extremely hard to compute all data in once. Hence, it is required to split the dataset to compute in a sequence. In this regards, the batch size means how much data should be categorized in once. The characteristics of the dataset are different for all kind; it is important to conduct the iteration process to find the optimum batch-size. Not only that, epoch number is also can be a critical factor to adjust the neural network. It helps to observe the optimum times of computation should be repeated to find the optimum output. For example, if someone is walking on the strange street, it is required to walk in the street a few times to get used to the place. The epoch means how many repeating processes is optimum to build a most accurate model.

3.2.3 Validation methods

It is a critical process to validate the neural network after the end of the process. Firstly, the cross-validation and separated data sets are used to validate in the first step for the validation. The whole data set is split into two categories; train and test data set. First, the train data set was evaluated as 70, 80 and 90% of the total data. According to the existing method and accuracy, about 80% of the data was used as train data. In addition, the remaining 20% data was not used to build the neural network but was used as an index to evaluate the accuracy of the created neural network configuration. It is difficult to validate

the accuracy of the neural network that was created, and problems such as overfitting occurred, so the data was divided at a ratio of 8:2. Therefore, the first validation technique is using 20% data which is not used for the neural network for validation.

The second technique is cross-validation. It is not further different from the previous technique. After splitting the dataset at 8:2 ratios, the test data set should be shuffled due to the reason of flexibility. Therefore, various rows of test data sets are randomly chosen and evaluated again to find the optimum neural network. It is a fundamental skill to choose the ratio and test dataset to decide the test dataset.

After complete the create a neural network, test data set is evaluated with several statistical methods such as root mean squared error (RMSE) or mean absolute percentage error (MAPE). However, most of the data is scaled down in a region of 0 to 1, it was not affordable to use MAPE due to the result of MAPE can be diverged to infinite when the data result is in a vicinity of 1. In the case of mean absolute scaled error (MASE), it is effective to compare the data between transient and steady data. However, the purpose of the neural network is delivering the outcome in steady-state, so it is excluded. Therefore, the root mean squared error method is used to evaluate the neural network. In the case of RMSE, it also has weakness such as Scale-dependent error, but most of the data is converted with the specifically designed scalers, it is an optimum

method to evaluate it. Fig 3.2 shows the total processes for building a neural network in flow chart. Fig 3.3 shows the comparison between the forward and backward neural networks which are suggested for this study.

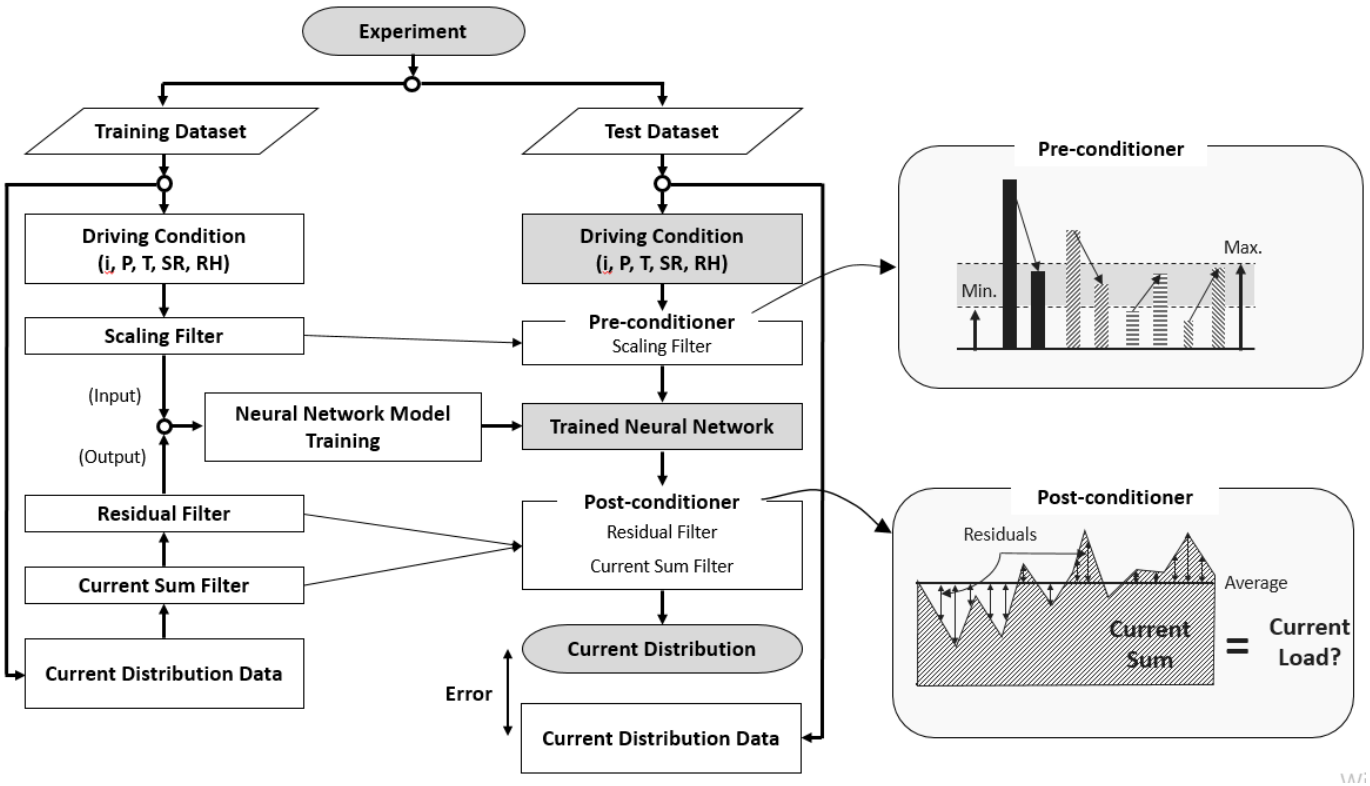

Figure 3.2 Flow chart for building a neural network

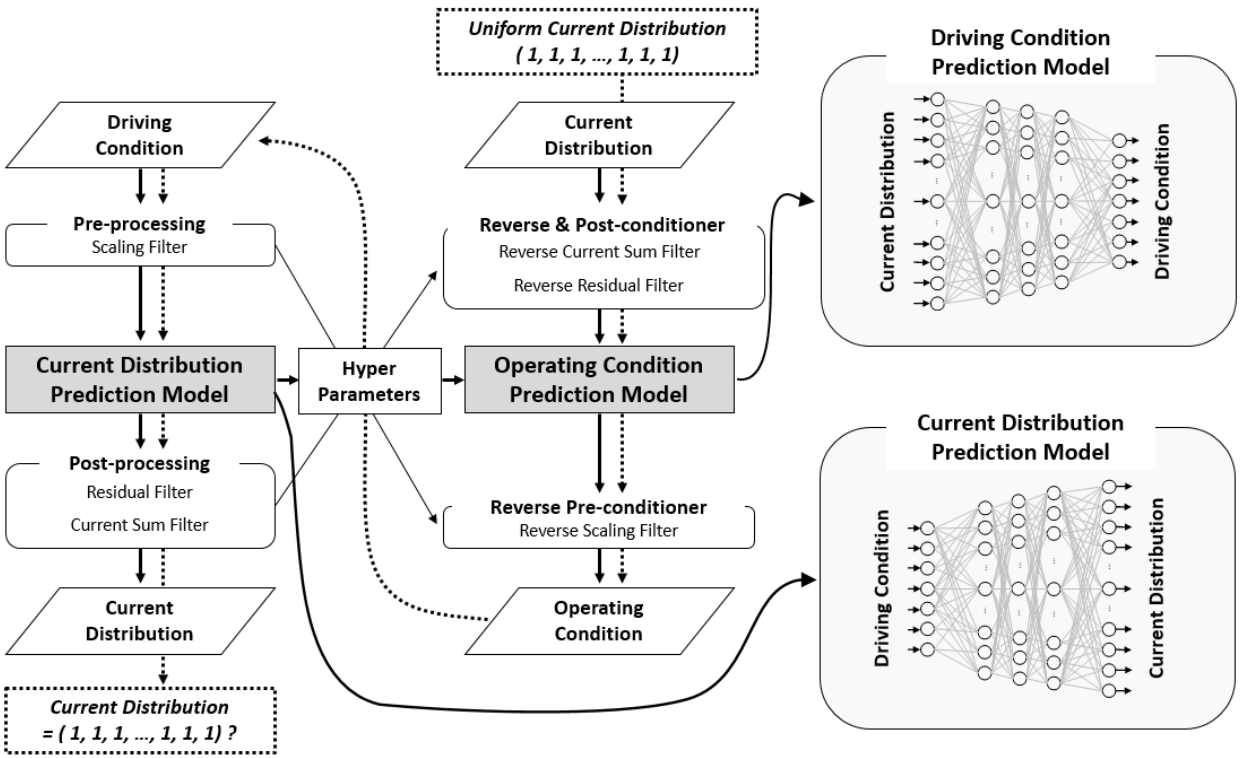

Figure 3.3 Algorithms of forward and backward neural networks

3.3 Results and discussion

3.3.1 Predict current distribution

Prediction on the current density distribution under various operating conditions is the primary objective to use neural networks. It is a data-based statistical model, so experiment data from the previous studies by Y.S Kim et al; and chapter 1 is used to build a neural network. Due to limitations of the neural network, if the prediction result is in the out of dataset, the accuracy could be converged or diverged.

a)Temperature and Pressure

Firstly, the created neural network is used to predict the current distribution when temperature and pressure are changed. Fig 3.4 shows the prediction results from the neural network. The predicted temperature range is between 20 to 70. Prediction result shows extremely low current density in the outlet region at the low-temperature range. The reason for this is the flooding effect is a dominant factor in the low-temperature region. As increasing the temperature relieves the flooding effect and the uniformity is increased as shown in Fig 20.

In the case of pressure, it does not influence the current distribution as a dominant factor. As seen in Fig 3.5, increasing pressure does not influence

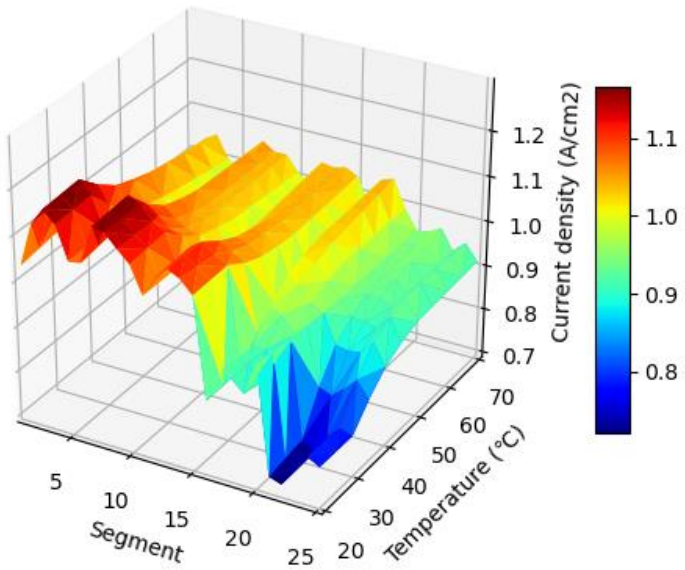

Figure 3.4 Variation of current distribution with temperature changes

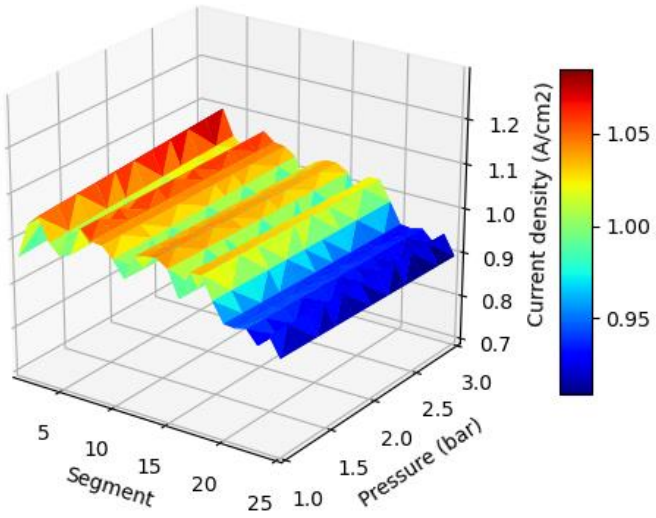

Figure 3.5 Variation of current distribution with pressure changes

the distribution even though it is pressurized above than 3 bar. However, this result shows under 65°C and 80% RH condition. Therefore, the reference condition is not suitable to observe the effects of pressure on the current distribution.

To scope the variation of uniformity, standard deviation contour is plotted as seen in Fig 3.6. As seen in the figure, temperature increment reduces the standard deviation, but the pressure increasing does not influence on the uniformity dominantly. However, in the low-temperature region, the increasing temperature seems to efficient to remove the water and flooding effects. The standard deviation at 20°C has the highest standard deviation among all cases, but increasing pressure reduces it in 30%.

b) Air flowrates (Cathode SR)

Due to fuel providing does not influence on the power output and current density distribution, only air providing is controlled to get a prediction. Fig 23 shows the variation of current density distribution by changing the air flowrates. Due to mass transfer loss, the current density at the inlet area is relatively high than the outlet region. However, increasing the air providing reduces the degree of mass transfer loss and finally, it has reduced as seen in Fig 3.7.

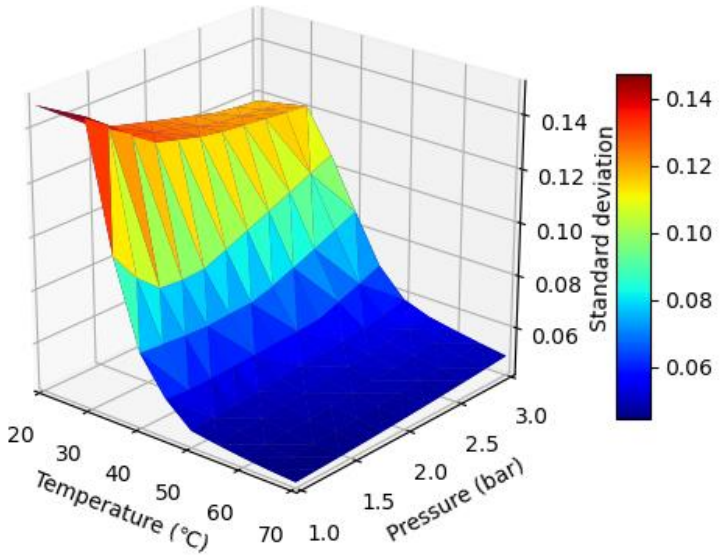

Figure 3.6 Distribution of standard deviation when temperature and pressure change

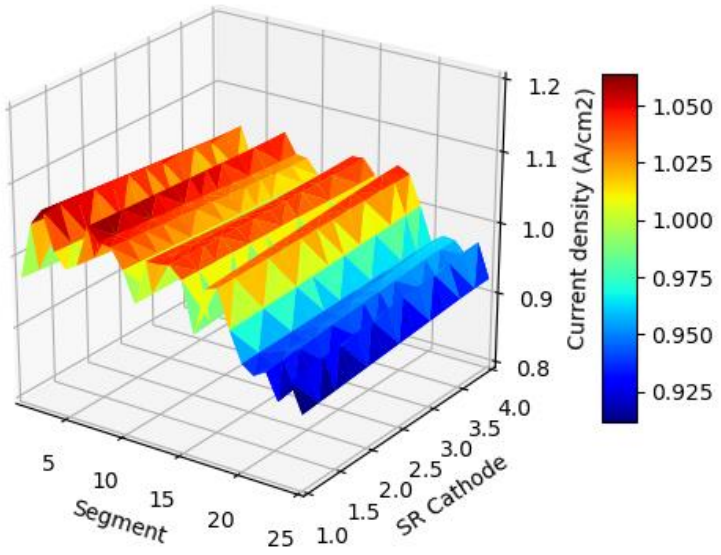

Figure 3.7 Variation of current distribution with air flowrate changes

c) Relative Humidity (RH)

In the case of relative humidity condition, the humidity of anode and cathode is processed separately. Fig 3.8 and 3.9 show the variation of the current density distribution of anode and cathode sides. As seen in the figure, increasing fuel humidity does not affect the distribution. However, humidity in the air providing changes the uniformity a lot. Due to insufficient humidity at the cathode side, the current density is focused on the middle of flow-field. However, as increasing the air humidity assists to increase the current density at the inlet area by the fast reaction, and it enhances the uniformity of current distribution for the whole fuel cell.

Aside from current distribution, Fig 3.10 shows the effects of humidity on the standard deviation. As seen in contour, if the fuel cell is fully-dehumidified, uniformity is reached to the lowest point due to insufficient conditions to perform at inlet region. In this context, increasing the humidity led to a decrease in the standard deviation, and it reaches the optimum uniformity point in the vicinity of RH 80% for both sides. After then, the standard deviation is increased again due to the flooding effect at the fully humidified condition. Therefore, it can be regarded as RH 80% is an optimum humidity condition to maintain the uniformity in equal. In addition, we can also find cathode RH is further dominant than the degree of fuel humidification.

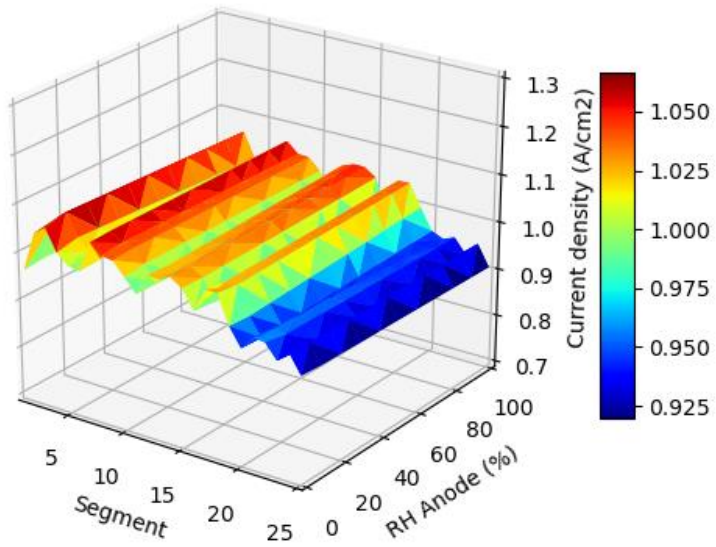

Figure 3.8 Current density distribution with humidity of fuel changes

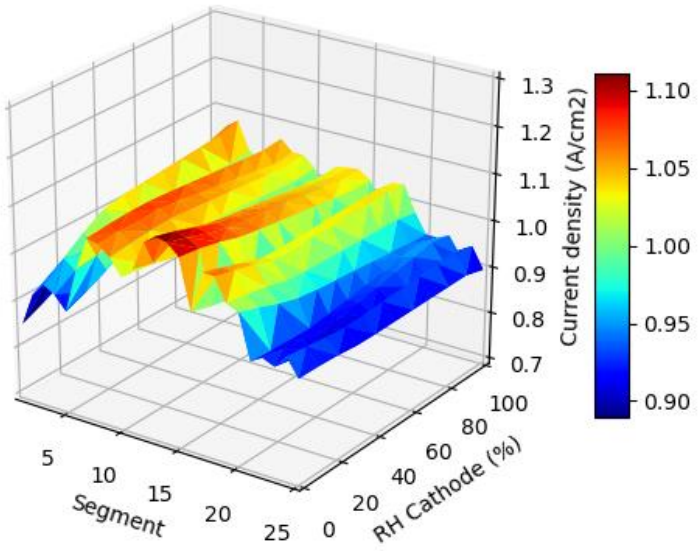

Figure 3.9 Current density distribution with humidity of air changes

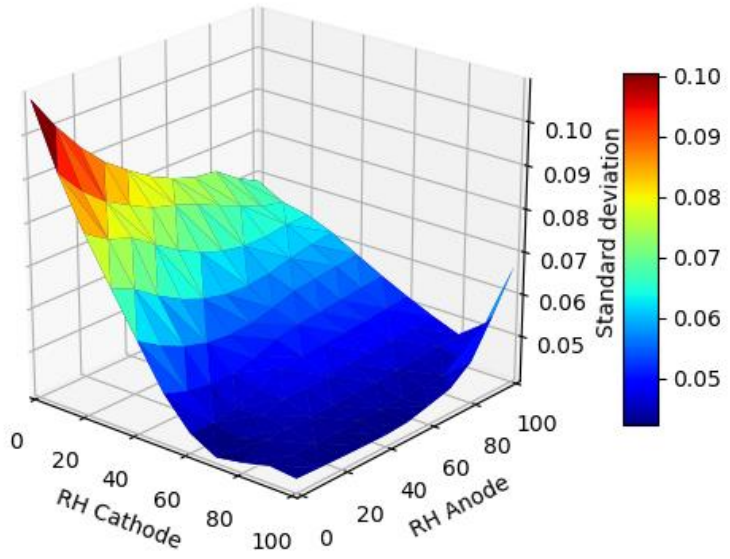

Figure 3.10 Distribution of standard deviation when relative humidity changes for both anode and cathode

3.3.2 Predict optimum experimental conditions

The second proposed method of using the neural network is to find the optimal operating conditions for PEMFC. As mentioned above, the performance and local current density of a fuel cell varies according to various operating conditions. Therefore, it is difficult to find and set the current distribution desired by the driver through numerical analysis or experiment. In addition, to alleviate this phenomenon when the characteristics change due to local degradation and so forth, the operating conditions must be adjusted before the operation. To this end, a method of searching for optimal operating conditions using neural networks has been newly studied.

Fig 3.11 below is the result of verifying the experimental conditions obtained using the backward neural network through a forward neural network. As can be seen in the figure below, most of the current density was uniformly distributed. Besides, Fig 3.12 compares the results of the reference operation conditions and the recommended condition which is suggested by the backward neural network. The reference condition is 65°C, 80% RH, fuel SR in 1.5, air SR in 2.0 and 1.0 bar. The below figure shows the current density for each line in the serpentine flow field. As can be easily seen, it can be seen that it is possible to operate with a much more uniform current density when operating under the proposed operating conditions through the neural network compared to the reference operating condition.

Table 4 shows the quantitative comparison between the forward neural network and backward neural network to find the minimum standard deviation. Even though the forward neural network is searched for most of the range of experiment parameters, it is difficult to cover all cases. Hence, the optimum uniformity found by forward one is around 0.04, and the average standard deviation by forward is up to 0.055. However, the backward neural networks found the average standard deviation as 0.0412 and the minimum is further lower to 0.025 which is the smallest standard deviation among all cases.

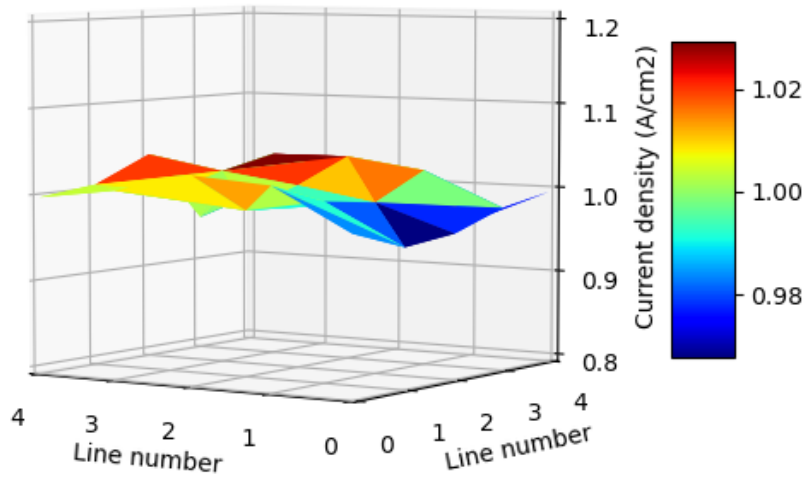

Figure 3.11 Current density distribution under the backward neural network suggested condition

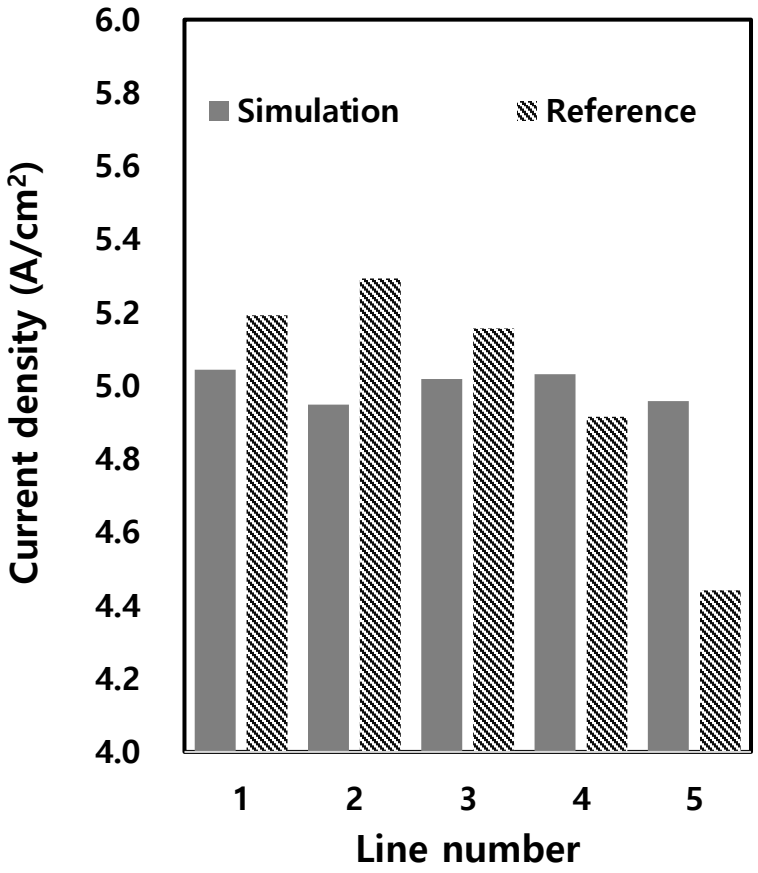

Figure 3.12 Comparison between the reference operating condition and neural network suggested condition

Table 4. Quantitative comparison to find the optimum uniformity of current density distribution

Neural networks		Average SD	Minimum SD
Forward	Temperature	0.12	0.057
	RH	0.075	0.043
	SR	0.055	0.046
	Pressure	0.062	0.058
Backward		**0.0412**	**0.025**

3.4 Summary

Due to durability and reliability is constantly in the limelight, it is necessary to study the augmentation techniques to extend the local durability of polymer electrolyte membrane fuel cell (PEMFC). However, the distribution of local current density can only be observed with a segmented fuel cell, and it is limited to experiment with operating parameters that go beyond 6 dimensions according to the conditions such as degradation. In addition, the analysis of local current density changes through numerical analysis approach faced problems of accuracy and computation time, so a new method was required to solve these problems.

Therefore, neural networks based on the statistical approach is used. First, a neural network was developed that can observe changes in current density when entering experimental conditions. To this end, data pre-processing techniques specifically proposed for fuel cells have also been devised. Through this, the current density distribution according to the experimental conditions can be adjusted with high accuracy within a range of tested condition. In addition, it was also possible to find a method to find operating conditions close to the desired current distribution, which is difficult to solve by numerical analysis.

As a result, this chapter introduced a bidirectional neural network-based modelling to improve the local durability of PEMFC. Through this, it is

possible to predict and control the internal local current density in the fuel cell. Therefore, one methodology was proposed to solve the durability problem that could be caused by imbalanced thermal shocks due to the low uniformity of the local current density.

Chapter 4. MEA degradation and current distribution with an accelerated stress test (AST)

4.0 Introduction

As the durability of PEM fuel cell is being a critical issue for the commercialization, various accelerate stress tests (AST) are suggested to observe the degradation. According to A. El-kharouf et al. there are several methods to degrade PEM fuel cell artificially. The accelerate degradation methods are mainly divided into three different parts; mechanical, chemical and thermal.

Firstly, mechanical degradation is normally occurred due to early failures of cracks in the membrane or pinholes. These can be resulted by several factors, such as elongation, tear strength and glass transition. Tnag el al. also conducted mechanical strength of Nafion membrane by mechanical stress cycling test, and it led to change the structure of membrane significantly, especially about pinholes.

In the case of thermal degradation, it can be effected on the changing on the characteristics of the membrane. When MEA works under high temperature or subfreezing temperatures, the structure of MEA can be changed. Therefore, the thermal degradation test can be experienced on and off cycling of heating or

freezing processes. Not only that, Jespersen et al. studied the degree of thermal degradation can be different from the material of membranes such as different degree of temperature tolerance. Therefore, it leads to hot spots when it works at a relatively high temperature.

Last but not least the case is chemical degradation. It can be referred to as ionomer damage that is resulted from carbon corrosion and platinum agglomeration/migration. It results in decrease in the membrane conductivity and change the local distribution of catalysts. Therefore, the total performance of fuel cell can be reduced in a result of decreasing conductivity and density of catalyst.

In this study, chemical degradation is used to study the change in current density distribution. Eom et al. studied over-potential degradation cases [10]. This study shows the performance reduction when the cycle is repeated for 20 times when the fuel cell is experienced at 1.4 V over-potential. He compared the carbon-based bipolar plates and other materials to observe the severity of degradation according to the types of material.

4.1 Experimental setup

4.1.1 An additional instruments

There are several instruments are required to conduct the accelerate stress test (AST) about the reverse-potential cycle. Most of the components are not tremendously different from the previously used segmented fuel cell system. Mainly three instruments are added to the previous system which is Agilent power supply, rely switch and NI voltage input module. The below system shows a schematic diagram of a modified auxiliary system. The programmed Labview transmits the signal to the DAQ in every 6 minutes to switch the circuit to the power supply, whilst power supply constantly supplies 1.5 V potential to the relay switch. Therefore, the reverse-potential applied to the fuel cell in every 6 minutes automatically as a charging process.

4.1.2 Experiment cases and conditions.

According to previous studies, the fuel cell can be experienced over-potential when it is under start/stop the cycle or stop for a long period. Therefore, the accelerated stress cycle consists of 6 minutes of over-potential step and another 3 minutes of open-circuit voltage (OCV) condition as seen in Fig 4.2 The used cycle for the experiment is referenced by the previous study [10].

As mentioned before, the reverse-potential causes degradation due to carbon corrosion and agglomeration/migration of loaded platinum catalysts on the membrane electrolyte assembly (MEA). Below equations show how degradation is processed.

$$C + 2H_2O \rightarrow CO_2 + 4H^+ + 4e^- \quad \text{.....[Carbon corrosion]}$$

$(E^0_r = 0.207\ V_{RHE})$

$$Pt2 + 2e^- \rightarrow Pt \quad \text{.....[Pt migration / agglomeration]}$$

$(E^0_r = 1.12\ V_{RHE})$

Firstly, carbon structure on the MEA is destroyed by over-potential cycle as shown in the above equation. Especially, the water is contented in the MEA, it could be regarded as the degradation will be progressed further seriously in fully humidified condition or under flooding effect. Therefore, the main idea of this research is from the water contents and local degradation. The experiment conditions are RH 80% and RH 40%, and the comparison between them is focused on the degree of degradation of the whole fuel cell and locally different degradation observed by the segmented fuel cell. The abovementioned over-potential cycle is applied for both humidity conditions until 20th cycles. However, the degradation occurred slowly in the RH 40% condition, so it was measured until the 30th cycle after the 20th cycle.

In addition, to compare the degree of degradation between inlet and outlet region, several additional instruments are used such as Electrochemical Impedance Spectroscopy (EIS), Scanning Electron Microscope (SEM), Energy Dispersive Spectrometry (EDS). In the case of EIS, it is conducted in every 5^{th} cycle after measured IV curves, and the SEM image is taken at the end of the degradation cycle. The primary purpose of EIS is measuring the variation of resistivity of the membrane after degradation. Due to corrosion and agglomeration of loaded catalysts, charge transfer loss is increased. Therefore, resistivity is observed to study the degree of degradation. In the case of SEM, it is required to see the local structures of the membrane by magnified images to verify the results, so it is conducted. Lastly, EDS is used to compare the fresh MEA and aged MEA quantitatively, so it shows the amount of carbon and platinum on the MEA, but it only shows the relative quantity of catalysts between them due to limitations.

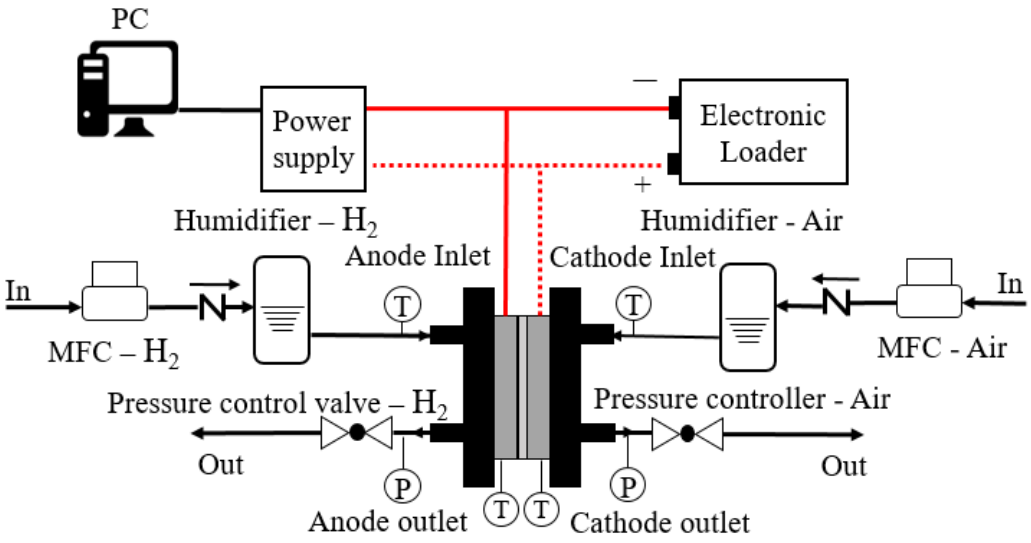

Figure 4.1 Schematic diagram of experimental system

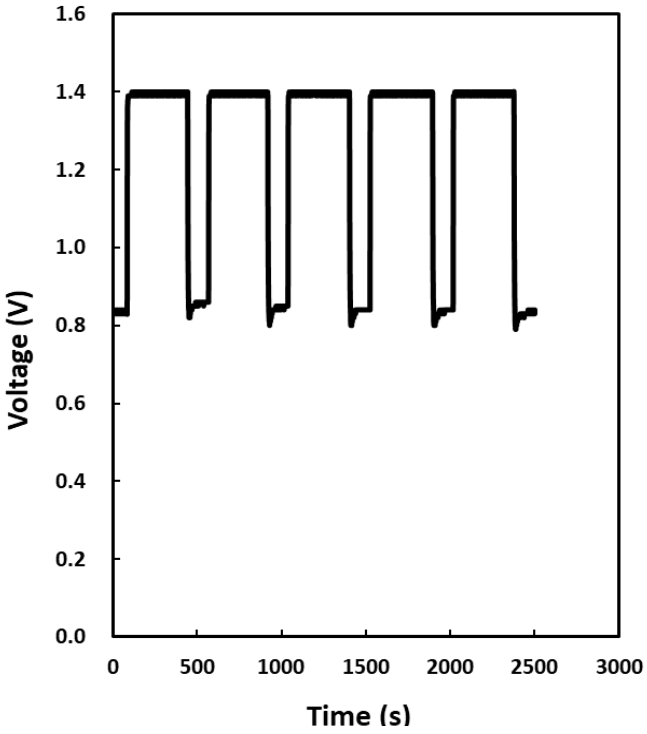

Figure 4.2 Reverse-potential cycle period and process

Figure 4.3 Used power supply to load the reverse-potential, Agilent Power Supply

4.2 Results and discussions

4.2.1 RH 80% condition

The first tested RH condition is 80% for both sides. Due to relative high humidity condition, the degradation is processed in quickly. The Fig 4.4 and 4.5 show the performance decrement along with the degradation cycling. As seen in the figure, the maximum power output is decreased about 5% to 8% in every 5^{th} cycle. After 20^{th} cycle, the power output is decreased to 9 W from the 13 W, so it decreased about 30% in 20 cycles. This is because of that the increasing of activation loss and concentration loss as seen in IV curves. Every cycle leads to drop the concentration loss remarkably especially at the high current region.

It is necessary to observe the reason of degradation further in detail with a segmented fuel cell. Fig 4.6 shows the variation of current density distribution along the every 5^{th} stress cycles. As seen in the figure, the current density at the outlet region is decreased up to 1.87%, whilst 2.9% increasing in inlet region. The given line 1 to 5 is delivered from the below figure 33 which is shown the splitting of serpentine flow field by lines. In overall, current density at the inlet region is increased up to 4% whilst about 4% decreasing in the outlet region. The reason for this is outlet region is experienced the flooding whilst under operation, so the higher water amount at the outlet region accelerates the degradation. In addition, it is tested under constant current condition, required amount of current is shifted to the inlet region where is less degraded.

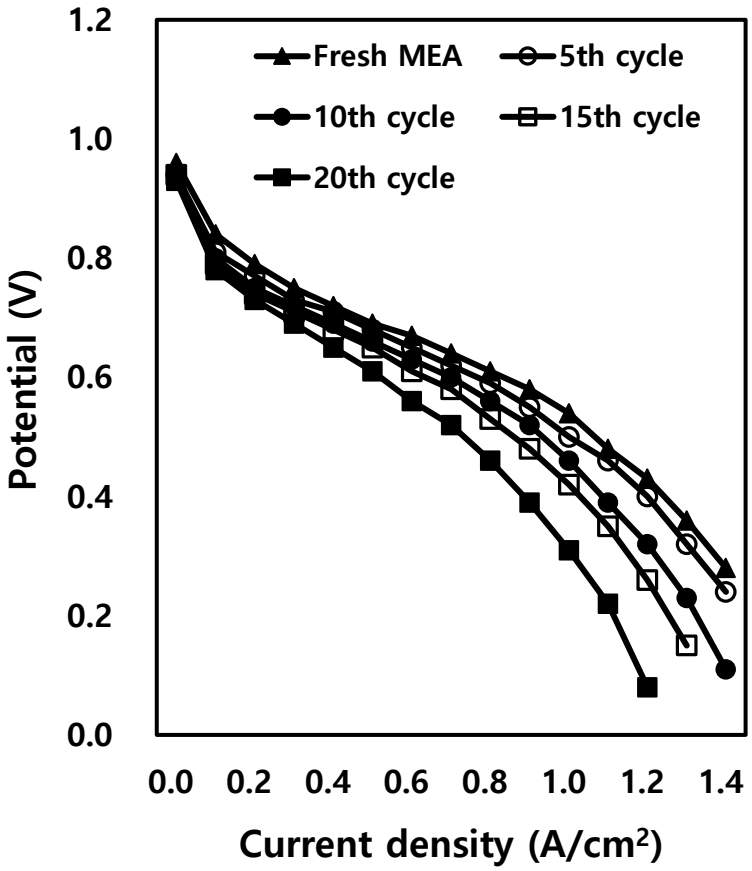

Figure 4.4 Changes of IV curves along with degradation cycles

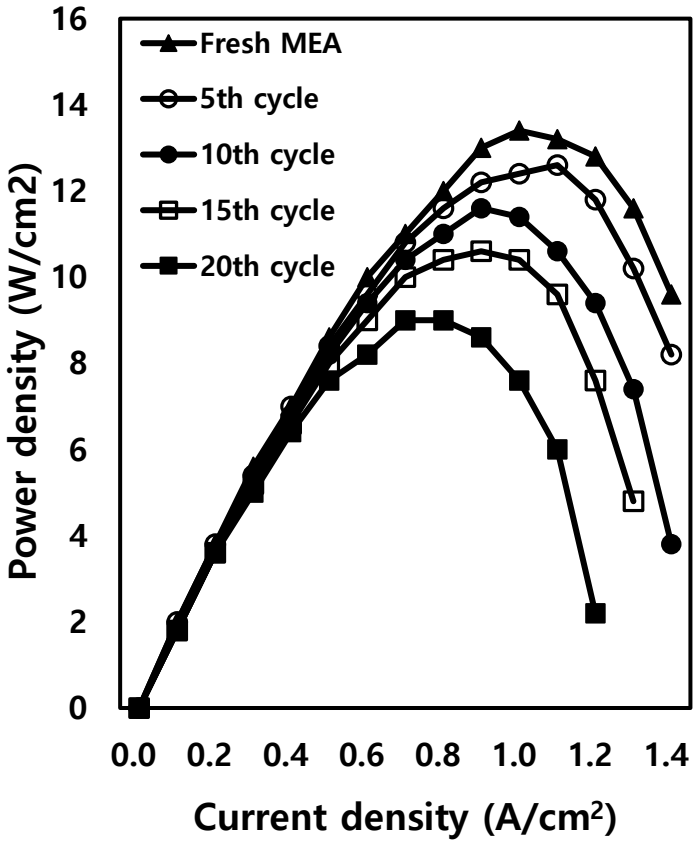

Figure 4.5 Changes of IP curves along with degradation cycles

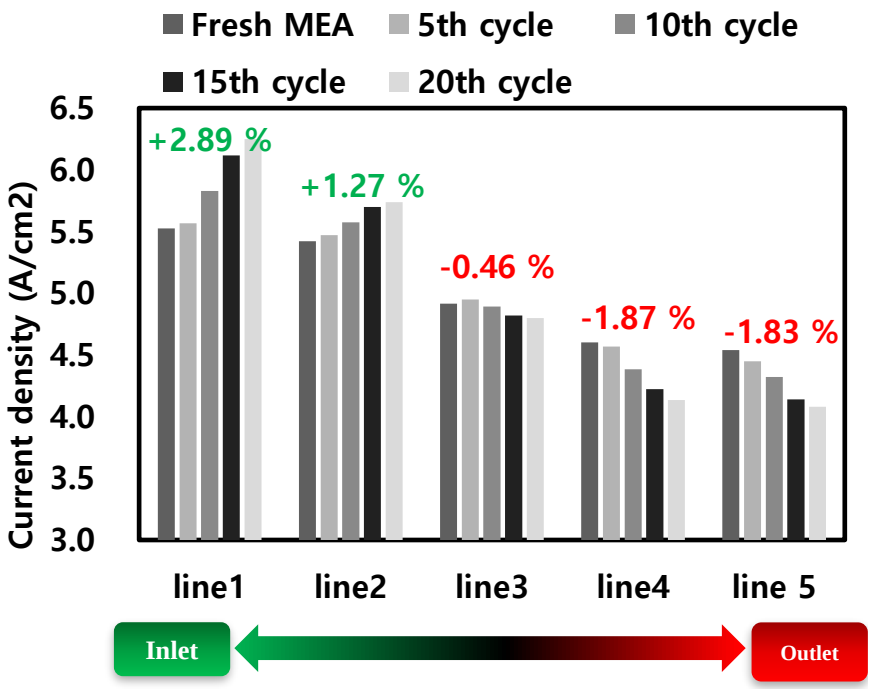

Figure 4.6 Variation of current density distribution when fuel cell experiences degradation by lines

To scope this phenomena, EIS is firstly used to measure the variation of resistivity of cycling. Fig 4.7 shows the resistivity changes in the low current region which is mainly purposed to scope the activation loss. The below figure 36 is conducted under high current region to focus on the concentration loss. Due to the radius of concentration loss is much bigger than the radius of activation loss, EIS result of concentration loss can be over-lapped the activation loss results. Therefore, it is required to set the current level to low, 8A, to observe the activation loss. As seen in Fig 4.7 and 4.8, the radius of semi-circle is increased along with the cycling, so it can be regarded as the activation loss increased due to the insufficient catalysts and destroyed membrane layers. EIS test is conducted from the 20k Hz to the 650m Hz. It is started from the higher hertz region to the lower hertz region, and the higher hertz is affordable to measure the Ohmic loss and scan the activation loss and concentration loss in a descent order.

To see the membrane in magnified view, SEM and EDS test is additionally conducted. Figure 37 shows the thickness of cathode catalyst layer of fresh MEA. It was 12 ㎛ before the degradation, but it is thinned after the test to 6 ㎛. It is necessary to magnify the SEM image further in detail. Hence, the SEM image is zoomed in 1 ㎛ scale as seen in Fig 4.9. It is clear to see the loaded platinum and carbon are in the shape of clear structures. However, after 20^{th} cycle of stress cycle under 80% RH condition, the shape of catalyst layers

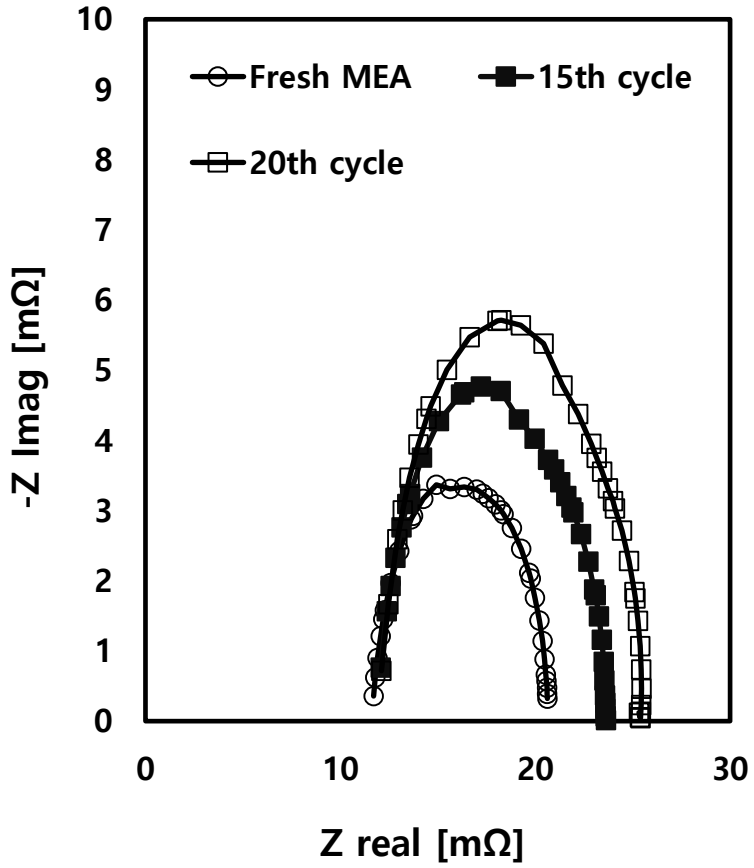

Figure 4.7 EIS on 0.32 A/cm^2 (low current region, RH = 80%)

¿

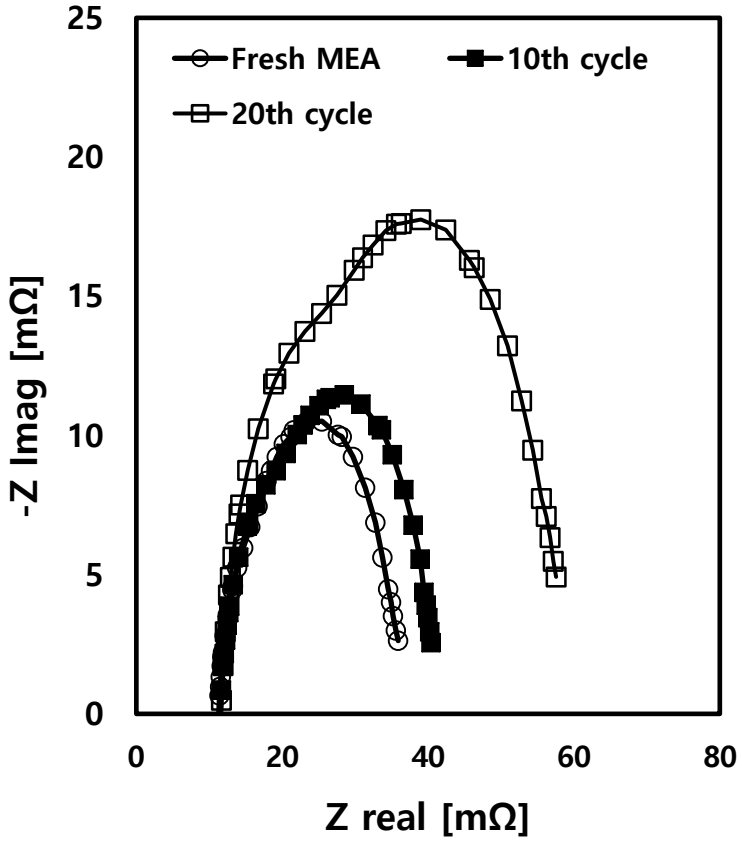

Figure 4.8 EIS on 0.96 A/cm^2 (high current region, RH = 80%)

is totally different. As seen in middle SEM image in Fig 4.10, platinum and catalyst layer is partly agglomerated in the surface of it. However, most of catalysts are agglomerated at the outlet region as seen in the below figure. In case of EDS, it shows the relative quantity of components in the MEA, and it is easily to find the amount of carbon is decreased sharply.

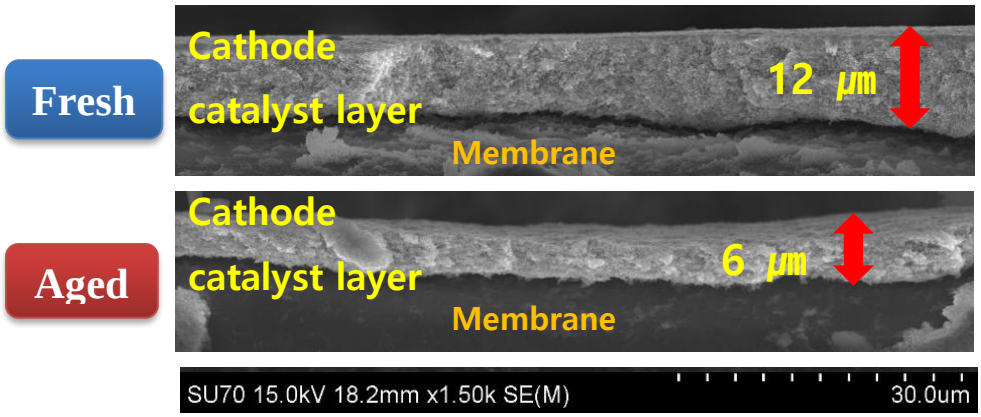

Figure 4.9 SEM image to compare the reduction in thickness of cathode catalyst layer after degradation

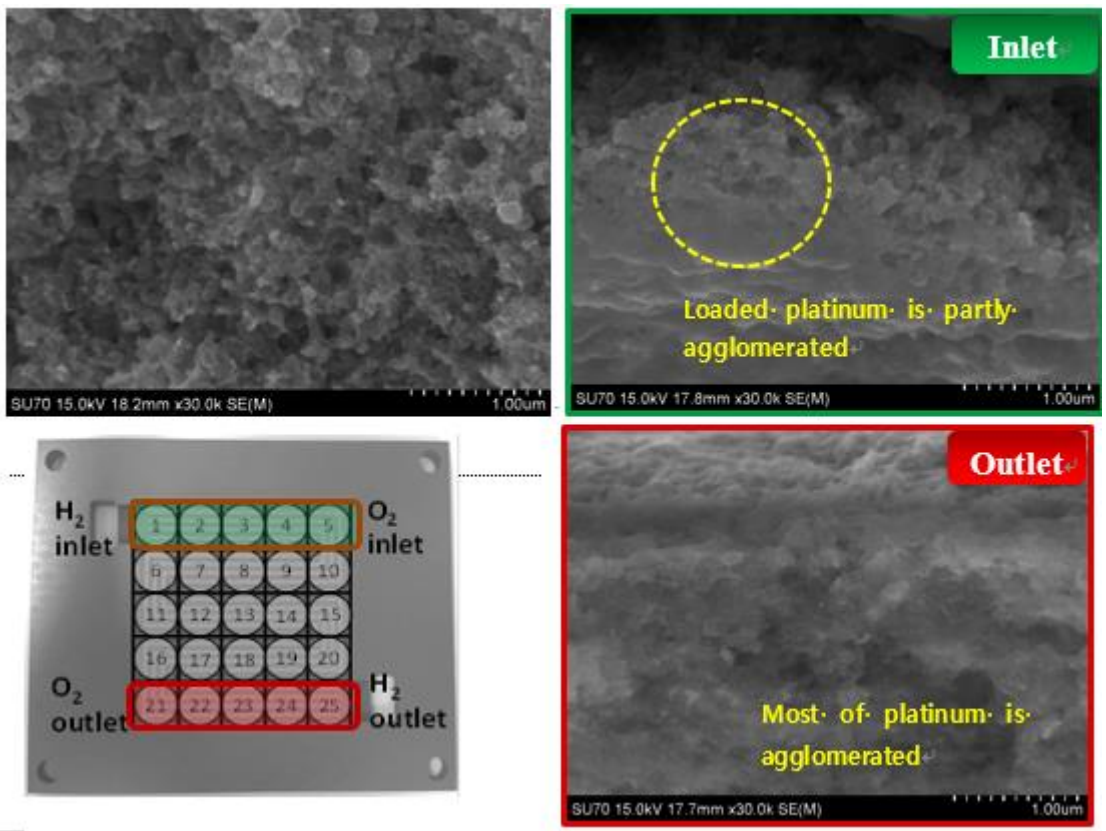

Figure 4.10 SEM images at the inlet and outlet regions after degradation cycles

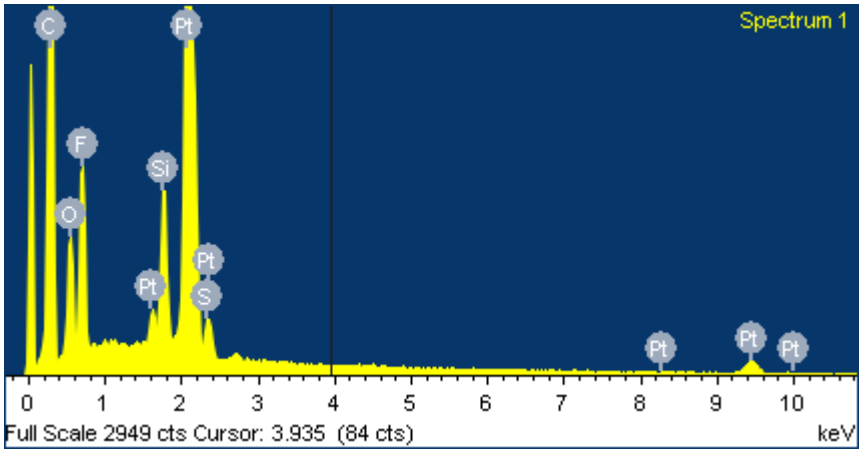

Before cycling

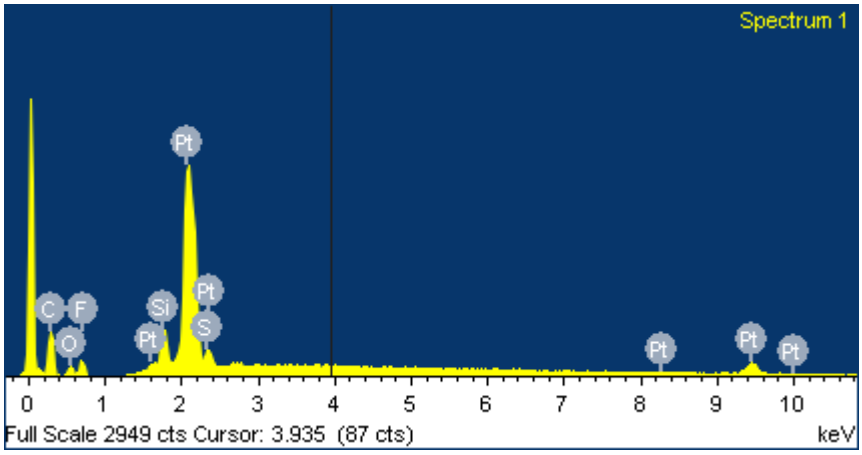

After cycling

Figure 4.11 EDS results to compare the amount of carbon in the MEA

4.2.2 RH 40% condition

The condition of RH 40% is tested as a second case. Due to relatively low humidity condition, the degradation rates are much slowly progressed. Fig 4.12 and 4.13 shows the variation of the maximum power output and IV curves. In the condition of 40% humidity, 20 cycles were also preferentially performed and compared with the previous condition. Compared to the previous condition, the performance decreased by about 8% in the low humidity condition. Subsequently, the degradation cycle was conducted until the 30^{th} cycle, but the overall performance is reduced by about only 20%. Therefore, the degree of degradation at low humidity is significantly weaker than the high humidity condition.

Fig 4.14 shows the variation of current density distribution under the low humidity condition. Overall trend of change is similar as high humidity condition; lower inlet region and higher outlet region. However, unlike the previous results, the degree and speed of degradation are significantly different. As can be seen in the figure, the change in the current density distribution was very small, but the current density distribution near the outlet due to the flooding effect and the tendency to increase near the inlet were similar with the previous condition. The reason for this is the flooding effect is not a critical factor in this case, and the dominance of humidity in the gas itself became much important.

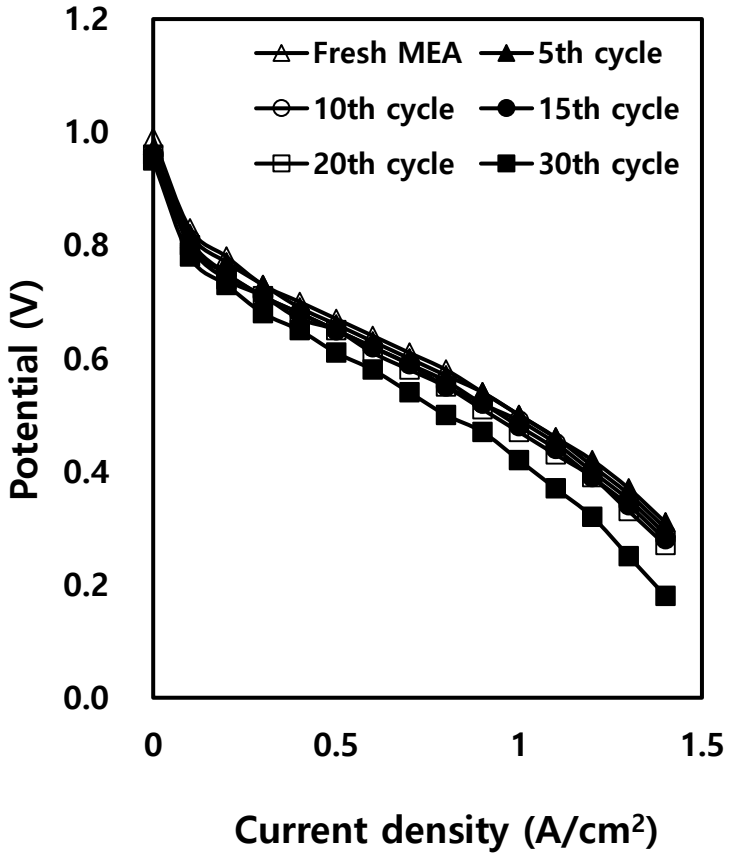

Figure 4.12 Changes of IV curves along with degradation cycles (RH=40%)

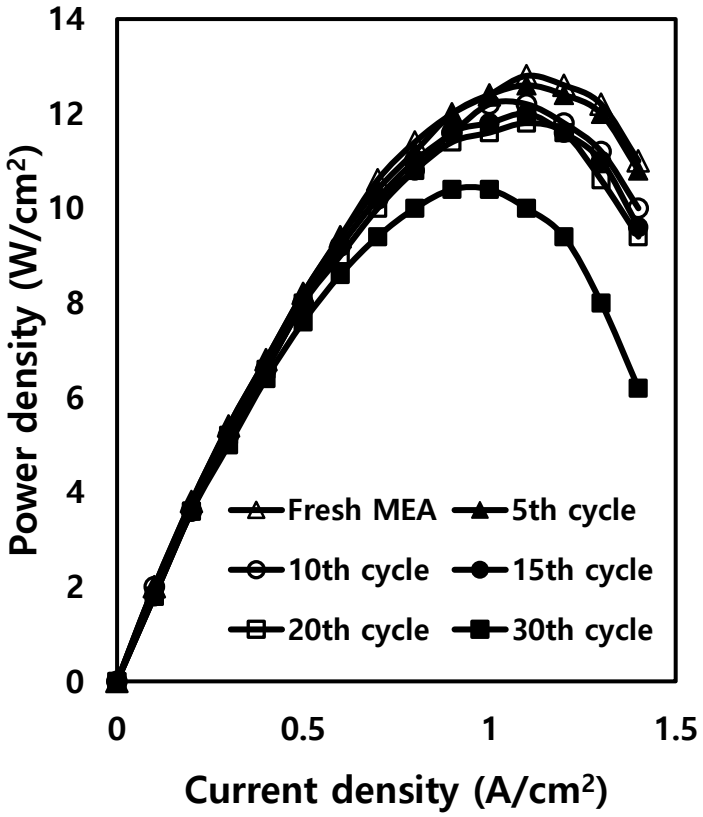

Figure 4.13 Changes of IP curves along with degradation cycles (RH=40%)

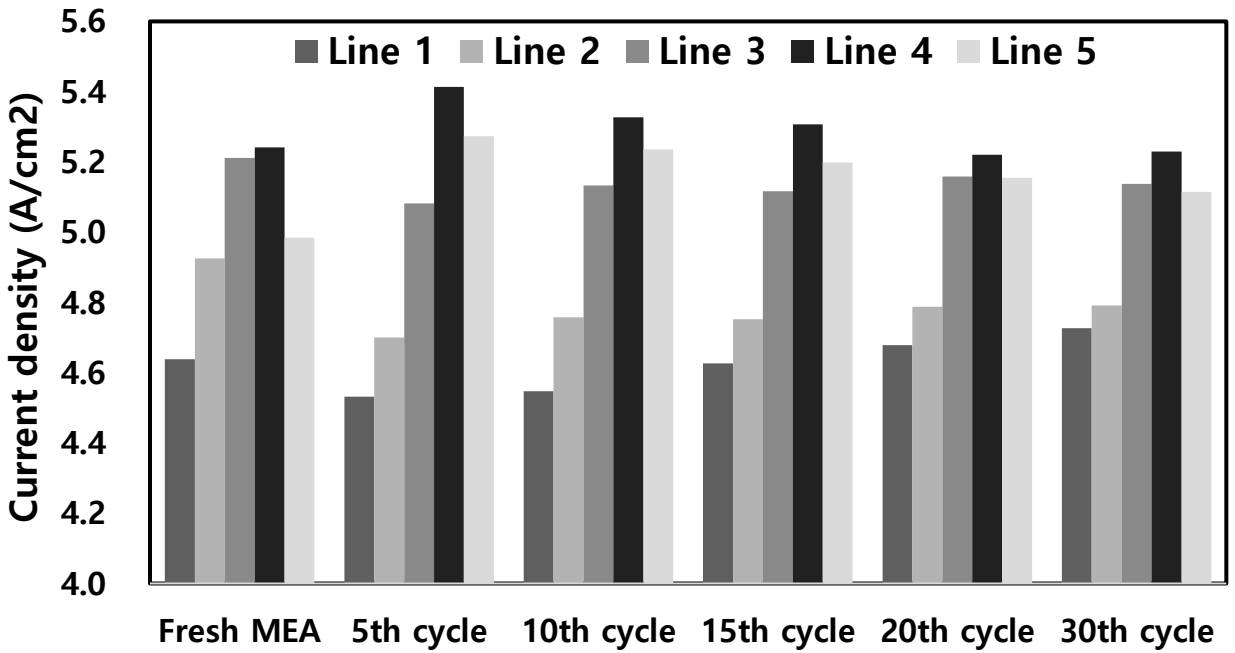

Figure 4.14 Variation of current density distribution with degradation by lines (RH=40%)

To compare the resistivity and reactivity of the membrane, the EIS test is also conducted for the low humidity condition as well. Firstly, the Fig 4.15 shows the EIS results under low current level, and it is regarded as the activation loss is increased along with cycles due to the radius of semi-circle is increased. In addition, if we compare them under high current region as seen in Fig 4.16, the mass transfer loss does not change a lot. Not only that, mass transfer loss can be compared with the previous EIS test result, and the radius of them under low humidity condition is much smaller due to the degree of flooding effects. Since the segmented fuel cell instruments have several auxiliary systems including hall effect sensor, the ohmic loss is plotted in the larger x-axis compared to the normal unit fuel cell. However, it is possible to observe them in relative comparison, and other charge transfer and mass transfer loss could be obtained in accurate results.

For the comparison of degree of degradation between the inlet and outlet region, SEM image is EDS test are also conducted. Inferred from previous results, it was expected that the catalysts would be much less severe than the high humidified cases. As shown, some degradation occurred, but no severe local degradation was found in the low humidity condition.

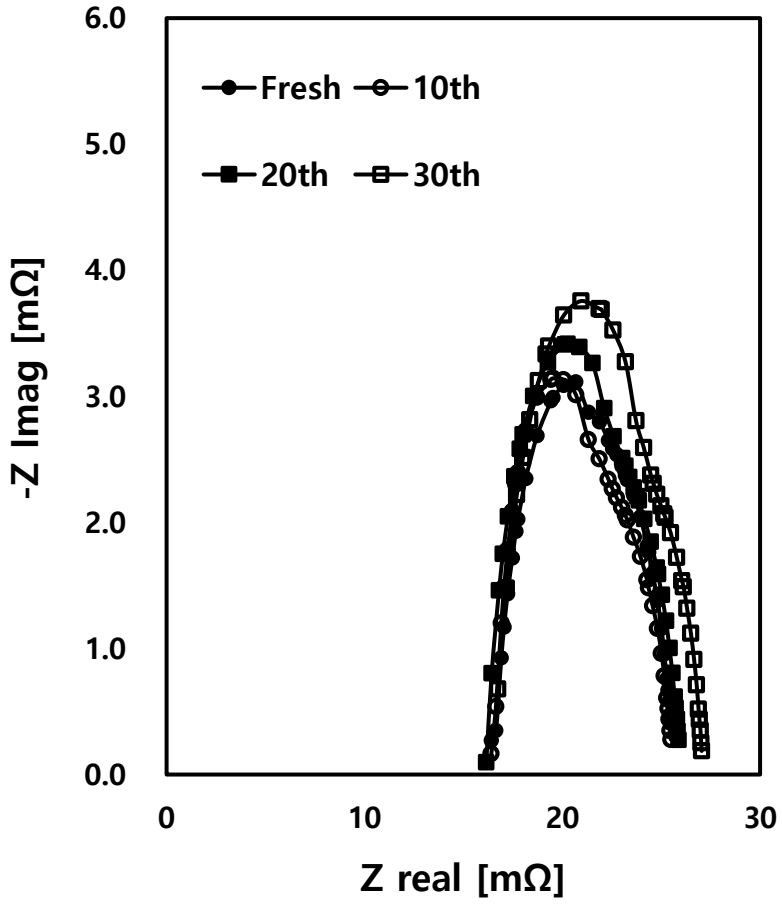

Figure 4.15 EIS on 0.96 A/cm^2 (high current region, RH = 40%)

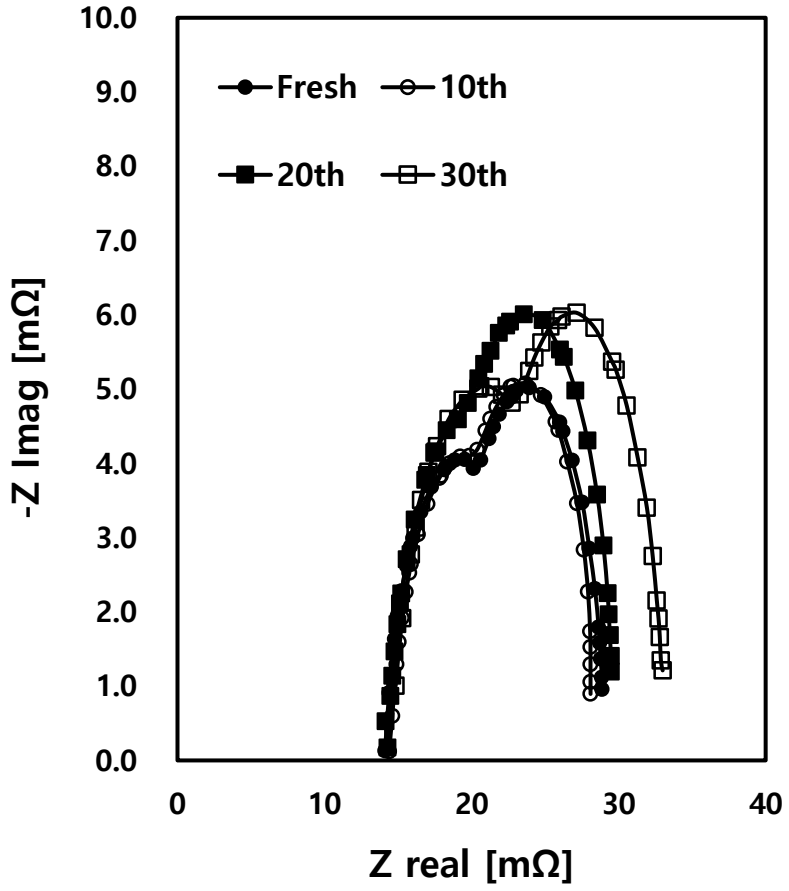

Figure 4.16 EIS on 0.96 A/cm^2 (high current region, RH = 40%)

Summary

In this chapter, the variation of current density distribution is observed when the fuel cell has experienced a degradation. The accelerated degradation method introduced is greatly influenced by the degree of hydration. Therefore, experiments were conducted under two different humidity conditions for a reverse voltage condition that could occur when starting/stopping or leaving the cell to stop for a long time. In particular, because the local water distribution is different due to flooding, the experiment was conducted with the segmented fuel cell that the degree of degradation will be different at the inlet and outlet. Among the two experimental conditions, it was found that in the high-humidity situation, severe degradation occurred at the outlet region with high water distribution. In low-humidity conditions, degradation also occurred at the outlet region, but the degree was not as severe as high humidity condition.

When designing the fuel cell membrane that operates in the high-humidity condition, it is necessary to design taking into account the degree of catalytic corrosion and locally different degradation especially at the outlet region. From the previous research, it is a critical factor to determine the degree of degradation at frequent stop/start conditions, it is required to design the corrosion resistivity with humidity condition when manufacturing the MEA.

Chapter 5. Conclusions

As fuel cells have entered the commercialization stage, research on reliability and durability has been spotlighted. Therefore, this study explored the phenomenon and degradation due to the imbalance of current density occurring in the polymer electrolyte membrane fuel cell (PEMFC). To this end, a segmented fuel cell is used to measure the local current densities depending on the position on the flow-field.

In the first study, changes in current density distribution under different conditions were studied. Temperature, humidity, flow rate, etc. were set as variables to derive local current density change and uniformity accordingly. In addition, research on performance has been proposed for operating conditions that consider both the maximum output condition and optimum uniformity.

Second of all, neural network based modeling is conducted to suggest a new type of prediction model for the current density distribution. Not only that, another type of modeling is also studied which is optimized for giving a suggestion to operate a fuel cell under uniform distribution. For them, several data preprocessing techniques are newly suggested for the unit fuel cell, and the modeling for finding an optimum operating condition is also newly proposed in this study. The accuracy and precison of the designed model is validated by existing validation method, and the backward neural network is

also verified by forward neural network which is designed for the forward neural network. The accuracy and error rates are convered into less than 2 %, and the suggested operating condition shows a minimum standard deviation. Therefore, this chapter showed high accuracy by incorporating the neural network in the field of fuel cells.

In the third chapter, changes in the current density distribution are observed when the fuel cell degrades. In order to shorten the experiment time, a reverse voltage accelerated degradation technique is introduced. Reverse voltage acceleration is a cycle in which reverse voltage is applied at regular cycles, which may occur when starting/stopping a fuel cell or leaving it for a long time. At this time, because moisture and water content are important factors for the rates of degradation, the experiment was conducted by dividing the humidity conditions into 40% and 80%. In addition, since the moisture content is different at the inlet and outlet regions, the degree of degradation according to the local spots were compared with the segmented fuel cell. To verify this, instruments such as EIS, SEM and EDS were also used.

In conclusion, this study observed the current density distribution inside the fuel cell. From the basic research according to the operating conditions to the distribution changes during degradation, it was observed through experiments. In addition, a neural network-based modeling method is proposed to efficiently

manage it. Therefore, in this study, research is conducted to prevent local degradation of the fuel cell.

References

[1] IPCC, 2018, IPCC Special Repot on Global warming of 1.5°C.

[2] United States Environmental Protection Agency, 2019, Inventory of U.S. Greenhouse Gas Emissions and Sinks 1990-2017

[3] ZHAO, Li, et al. Dynamic performance of an in-rack proton exchange membrane fuel cell battery system to power servers. International Journal of Hydrogen Energy, 2017, 42.15: 10158-10174.

[4] BIZON, Nicu. Tracking the maximum efficiency point for the FC system based on extremum seeking scheme to control the air flow. Applied energy, 2014, 129: 147-157.

[5] MATRAJI, Imad, et al. Comparison of robust and adaptive second order sliding mode control in PEMFC air-feed systems. International Journal of Hydrogen Energy, 2015, 40.30: 9491-9504.

[6] Fang-Bor Weng, C.-Y. H. C.-W. L., 2010. Experimental investigation of PEM fuel cell aging under current cycling using segmented fuel cell. Hydrogen energy, 제 35, pp. 3664-3675.

[7] Jing Shan, R. L. S. X. e. a., 2016. Local resolved investigation of PEMFC performance degradation mechanism during dynamic driving cycle. Hydrogen Energy, 제 41, pp. 4239-4250.

[8] K. Belmokhtar, M. D. K. A., 2014. PEM Fuel Cell Modelling Using Artificial Neural Networks (ANN). International Journal of Renewable

Energy Research, 3(4).

[9] Kui Chen, S. L. A. D., 2018. Proton Exchange Membrane Fuel Cell Degradation and Remaining Useful Life Prediction based on Artificial Neural Network. Paris, France, 7th International Conference on Renewable Energy Research and Applications.

[10] Kui Chen, S. L. A. D., 2019. Degradation prediction of proton exchange membrane fuel cell based on grey neural network model and particle swarm optimization. Energy Conversion Management, 195, pp. 810-818.

[11] KwangSup Eom, E. C. e. a., 2012. Degradation behavior of a polymer electrolyte membrane fuel cell employing metallic bipolar plates under reverse current condition. Electrochimica Acta, Issue 78, pp. 324-330.

[12] N. Rajalakshmi, M. R., 2002. Evaluation of current distribution in a proton exchange membrane fuel cell by segmented cell approach. Power Sources, 112, pp. 331-336.

[13] Rui Lin, C. C. J. M., 2012. Optimizing the relative humidity to improve the stability of a proton exchange membrane by segmented fuel cell technology. Hydrogen energy, Issue 37, pp. 3373-3381.

[14] Y. Biecer, I. D. M. A., 2016. Maximizing performance of fuel cell using artificial neural network approach for mart grid applications. Energy, Issue 116, pp. 1205-1217.

[15] Bowen Feng, e. a., 2019. Study on the Uncoupling Characteristics of PEM Fuel Cell by Segmented Cell Technology. Electrochemical Science, Issue

14, pp. 2175-2186.

[16] Cong Yin, e. a., 2016. In situ investigation of proton exchange membrane fuel cell performance with novel segmented cell design and a two-phase flow model. Energy, Issue 113, pp. 1071-1089.

[17] Cong Yin, e. a., 2020. Study of internal multi-parameter distributions of proton exchange membrane fuel cell with segmented cell device and coupled three-dimensional model. Renewable Energy, Issue 147, pp. 650-662.

[18] Dietmar Gerteisen, e. a., 2012. EEffect of operating conditions on current density distribution and high frequency resistance in a segmented PEM fuel cell. Hydrogen Energy, Issue 37, pp. 7736-7744.

[19] Dong Liang, e. a., 2011. Behavior of a unit proton exchange membrane fuel cell in a stack under fuel starvation. Power Sources, Issue 196, pp. 5595-5598.

[20] Fang-Bor Weng, C.-Y. H. C.-W. L., 2010. Experimental investigation of PEM fuel cell aging under current cycling using segmented fuel cell. Hydrogen Energy, Issue 35, pp. 3664-3675.

[21] H Y Wang, W. Y. Y. K., 2014. Analyzing in-plane temperature distribution via a micro-temperature sensor in a unit polymer electrolyte membrane fuel cell. Applied Energy, Issue 124, pp. 148-155.

[22] Heng Shao, e. a., 2019. In-situ measurement of temperature and humidity distribution in gas channels for commercial-size proton exchange

membrane fuel cell. Power Source, Issue 412, pp. 717-724.

[23] Johan Ko, H. J., 2012. Comparison of numerical simulation results and experimental data during cold-start of polymer electrolyte fuel cells. Applied Energy, Issue 94, pp. 364-374.

[24] K. Belmokhtar, M. D., 2014. PEM Fuel Cell Modelling Using Aritificial Neural Netowkrs (ANN). International Journal of enewable energy research, 4(3).

[25] Kui Chen, e. a., 2019. Degradation prediction of proton exchange membrane fuel cell based on grey neural network model and particle swarm optimization. Energy Conversion and Management, Issue 195, pp. 810-818.

[26] Kui Chen, S. L., 2018. Proton Exchange Membrane Fuel Cell Degradation and Remaining Useful LIfe Prediction based on Artificial Neural Network. Paris, France, 7th International Conference on Renewable Energy Research and Applications.

[27] Kui Jiao, X. L., 2010. Cold start analysis of polymer electrolyte membrane fuel cells. Hydrogen Energy, Issue 35, pp. 5077-5094.

[28] Linfa Peng, H. S., 2020. Investigation of the non-uniform distribution of current density in commercial-size proton exchange membrane fuel cells. Power Sources, Issue 453.

[29] M. Schulze, E. G. S. S., 2007. Segmented cells as tool for development of fuel cells and error prevention/prediagnostic in fuel cell stacks. Power

Sources, Issue 173, pp. 19-27.

[30] Meiling Dou, e. a., 2011. Behaviors of proton exchange membrane fuel cells under oxidant starvation. Power Sources, Issue 196, pp. 2759-2762.

[31] N. Rajalakshnmi, M. R. K. D., 2002. Evaluation of current distribution in a proton exchange membrane fuel cell by segmented cell approach. Power Sources, Issue 112, pp. 331-336.

[32] Rui Lin, e. a., 2012. Optimizing the relative humidity to improve the stability of a proton exchange membrane by segmented fuel cell technology. Hydrogen Energy, Issue 37, pp. 3373-3381.

[33] Rui Lin, e. a., 2012. Optimizing the relative humidity to improve the stability of a proton exchange membrane by segmented fuel cell technology. Hydrogen Energy, Issue 37, pp. 3373-3381.

[34] S. Chevalier, C. J., 2018. Analytical solutions and dimensional analysis of pseudo 2D current density distribution model in PEM fuel cells. Renewable Energy, Issue 125, pp. 738-746.

[35] Sang-Min Park, e. a., 2009. Experimental investigation of current distribution in a direct methanol fuel cell with serpentine flow-fields under various operating conditions. Power Sources, Issue 194, pp. 818-823.

[36] Seung-Gon Kim, M.-J. K. Y.-J. S., 2015. Segmented cell approach for studying uniformity of current distribution in polymer electrolyte fuel cell operation. Hydrogen Energy, 35(40), pp. 11676-11685.

[37] Tatyana Reshetenko, A. K., 2019. On the distribution of local current

density along a PEM fuel cell cathode channel. Electrochemistry Communications, Issue 101, pp. 35-38.

[38] Tatynana V. Reshetenko, e. a., 2013. A segmented cell approach for studying the effects of serpentine flow field parameters on PEMFC current distribution. Electrochimica Acta, Issue 88, pp. 571-579.

[39] V. Lilavivat, S. S., 2015. Current Distribution Mappling for PEMFCs. Electrochimica Acta, Issue 174, pp. 1253-1260.

[40] Wei-Mon Yan, e. a., 2006. Effects of operating conditions on cell performance of PEM fuel cells with conventional or interdigitated flow field. Power Source, Issue 162, pp. 1157-1164.

[41] Y. Bicer, I. D. M. A., 2016. Maximizing performance of fuel cell using artificial neural network approach for smart grid applications. Energy, Issue 116, pp. 1205-1217.

국 문 초 록

연료전지는 다른 친환경 에너지에 비해 상대적으로 높은 에너지 변환 효율 및 저장성으로 인해 차세대 에너지원으로 각광받는 기술이다. 또한 자가발전을 위한 SOFC, 상대적으로 작동 온도가 낮아 운송 및 교통수단에 사용되는 PEMFC 등 다양한 종류의 연료전지가 여러 산업에서 응용 될 수도 있을 것으로 기대되어 많은 연구가 이루어 지고 있다. 또한 이미 상용화 단계에 들어선 연료전지의 내구성 문제가 중요시 되고 있기 때문에 본 연구에서는 연료전지 사형유로에서 상이한 전류 밀도로 인해 발생한 국소 온도구배에 의한 열화를 방지하기 위하여 전류밀도분포에 관한 연구를 진행하였다.

첫번째로는 연료전지가 운전 시 핵심적인 실험변수를 조정해 가며 실험을 진행하였다. 변수로는 작동 온도, 습도 및 수소 와 산소의 유량을 조정하며 실험을 진행하였다. 실험방법으로는 가로 세로 5cm, 넓이 25cm^2 의 반응 면적을 25 구간으로 나누어 전류밀도 분포의 변화를 살펴보았다.

두번째로는 인공신경망을 이용하여 연료전지의 운전 상태 분석 및 운전조건을 예측 및 조절 가능한 모델을 개발하였다. 이를 위해, 연료전지에 특화된 다양한 데이터 전처리 기법들이 적용 및 제안되었으며, 수치해석법으로는 어느정도

한계가 있는 전류밀도분포 예측 모델도 개발되었다. 뿐만 아니라 역방향 인공신경망을 이용하여 전류 밀도를 균일하게 맞추기 위한 운전조건을 제시하는 방법을 새롭게 도입하였고, 이를 모델링을 통해 검증하였다.

세번째로는 연료전지가 열화 되었을 때 발생할 수 있는 전류밀도분포 변화에 대해 연구하였다. 이를 위해 가속열화기법이 도입되었고, 습도에 따라 열화 정도가 변화하는 현상을 관찰하였다. 습도에 따라 출구부근에서 더 큰 열화가 일어나는 것을 관찰하고 EIS, SEM 및 EDS 등을 사용하여 이를 증명하였다. 또한 이를 통해 열화가 일어났을 시 국부적인 열화의 가속을 줄이고자 운전 조건의 조절을 두번째 챕터의 인공신경망을 통해 제어하는 방식도 새롭게 제안되었다.

주요어: 고분자전해질막 연료전지, 분할연료전지, 사형 유로
전류밀도분포, 인공 신경망

학번: 2018-26130